DOI: 10.1534/genetics.106.057893

Glial and Neuronal Functions of the Drosophila Homolog of the Human SWI/SNF Gene *ATR-X* (*DATR-X*) and the *jing* Zinc-Finger Gene Specify the Lateral Positioning of Longitudinal Glia and Axons

Xuetao Sun, Tatiana Morozova and Margaret Sonnenfeld[1]

Department of Cellular and Molecular Medicine, University of Ottawa, Ottawa, Ontario K1H 8M5, Canada

Manuscript received March 3, 2006
Accepted for publication April 27, 2006

ABSTRACT

Neuronal–glial communication is essential for constructing the orthogonal axon scaffold in the developing Drosophila central nervous system (CNS). Longitudinal glia (LG) guide extending commissural and longitudinal axons while pioneer and commissural neurons maintain glial survival and positioning. However, the transcriptional regulatory mechanisms controlling these processes are not known. Previous studies showed that the midline function of the *jing* C_2H_2-type zinc-finger transcription factor was only partially required for axon scaffold formation in the Drosophila CNS. We therefore screened for gain-of-function enhancers of *jing* gain of function in the eye and identified the Drosophila homolog of the disease gene of human α-thalassemia/mental retardation X-linked (ATR-X) as well as other genes with potential roles in gene expression, translation, synaptic transmission, and cell cycle. *jing* and *DATR-X* reporter genes are expressed in both CNS neurons and glia, including the LG. Coexpression of *jing* and *DATR-X* in embryonic neurons synergistically affects longitudinal connective formation. During embryogenesis, *jing* and *DATR-X* have autonomous and nonautonomous roles in the lateral positioning of LG, neurons, and longitudinal axons as shown by cell-specific knockdown of gene expression. *jing* and *DATR-X* are also required autonomously for glial survival. *jing* and *DATR-X* mutations show synergistic effects during longitudinal axon formation suggesting that they are functionally related. These observations support a model in which downstream gene expression controlled by a potential *DATR-X*–Jing complex facilitates cellular positioning and axon guidance, ultimately allowing for proper connectivity in the developing Drosophila CNS.

DURING central nervous system (CNS) development, axons navigate long distances and are faced with both attractive and repulsive guidance cues that must be properly interpreted (Tessier-Lavigne and Goodman 1996). Many interneurons, whose cell bodies lie next to the CNS midline, must project their axons across the midline to form the commissural tracts. The "decision" of an axon to cross the midline of the Drosophila ventral nerve cord (VNC) and the vertebrate spinal cord depends on the differential response of axons to the midline repellent Slit and to the attractant Netrins (Seeger *et al.* 1993; Tessier-Lavigne 1994; Battye *et al.* 1999; Kidd *et al.* 1999; Long *et al.* 2004; Bhat 2005). After commissural axons cross the midline, they turn to fasciculate with the longitudinal tracts that run parallel to the midline and are repelled from the midline by Slit.

The ligand of Slit is Roundabout (Robo), which is located on the longitudinal glia (LG) and associated pioneer neuron growth cones adjacent to the midline (Kidd *et al.* 1998a; Kinrade *et al.* 2001). Signaling and cell–cell contact maintain the ipsilateral positions of both LG and connectives. In fact, Slit–Robo signaling cancels out the attraction of longitudinal axons to the CNS midline by Netrin–Frazzled (Bhat 2005). Commissureless (Comm) is a transmembrane protein that prevents the delivery of Robo to the growth cones, specifically in commissural neurons, allowing their axons to cross the midline (Tear *et al.* 1996; Keleman *et al.* 2002; Keleman *et al.* 2005). A downregulation of Robo by genetic means or by overexpression of *comm* results in an excess of axons at the CNS midline (Kidd *et al.* 1998b). Therefore, the differential localization of Comm, Robo, and Slit determines what directions navigating axons of the scaffold will follow. The Slit–Robo system is an important and conserved mechanism to establish cellular positioning and boundaries in the developing vertebrate and invertebrate nervous systems (Kidd *et al.* 1999; Rajagopalan *et al.* 2000a,b; Simpson *et al.* 2000a,b; Rasband *et al.* 2003; Barresi *et al.* 2005).

The relationship between neurons and glia and the formation of the Drosophila CNS axon tracts has been extensively studied by genetic and cell ablation methods (Hidalgo and Brand 1997, 2000; Booth *et al.* 2000).

[1]*Corresponding author:* Department of Cellular and Molecular Medicine, University of Ottawa, Ottawa, Ontario K1H 8M5, Canada.
E-mail: msonnenf@uottawa.ca

The longitudinal axon tracts are constructed by the extensions of four pioneer neurons (Bate and Grunewald 1981; Jacobs and Goodman 1989; Hidalgo and Brand 1997). To form a longitudinal fascicle, the dMP2 and MP2 pioneer neurons extend their axons posteriorly to contact the anteriorly projecting growth cones of the vMP2 and pCC neurons (Jacobs and Goodman 1989). In each hemisegment, LG act as mobile guideposts for the migrating axons (Hidalgo and Booth 2000). Early ablation of LG affects the joining of the descending and ascending pioneer growth cones and the subsequent fasciculation and defasciculation of pioneer and later follower axons (Booth *et al.* 2000; Hidalgo and Booth 2000). Despite the important guidance role of the LG, these cells depend on pioneer axons for their survival (Hidalgo *et al.* 2001; Kinrade *et al.* 2001). In addition, contralateral neuron cell bodies are needed for axon pathfinding onto the longitudinal connective (Whitington *et al.* 2004). The proper migration of follower glia in the fly optic lobe requires a preexisting photoreceptor axon scaffold (Hidalgo *et al.* 2001; Kinrade *et al.* 2001; Dearborn and Kunes 2004). Therefore, neuronal–glial interactions, in addition to guidance molecules, are instrumental during axon patterning (Oland and Tolbert 2002).

The *jing* gene was originally identified in two genetic screens for regulators of border cell migration in the ovary and for midline cell development during embryogenesis (Liu and Montell 2001; Sedaghat *et al.* 2002). During embryogenesis, *jing* transcripts accumulate in the CNS midline, adjacent neuroectoderm, brain, and trachea (Sedaghat *et al.* 2002; Sonnenfeld *et al.* 2004). In the CNS midline and trachea, Jing functions downstream of basic helix-loop-helix and PAS (Per–Arnt–Sim)-containing (bHLH-PAS) transcription factors to control tyrosine kinase signaling through the epidermal growth factor receptor (Egfr) and fibroblast growth factor receptor Breathless (Sedaghat *et al.* 2002; Sonnenfeld *et al.* 2004). In the CNS midline, *jing* is required for commissural and longitudinal axon formation but midline expression of wild-type *jing* does not completely rescue axon defects in mutants, suggesting that other functions of Jing contribute to axon tract formation (Sonnenfeld *et al.* 2004).

In a search for additional factors important for *jing* function, we carried out a genetic screen to identify genes whose function could modify that of *jing* in a gain-of-function (GOF) assay in the developing eye-imaginal disc. Seven third chromosome enhancer/promoter-tagged (EP) genes were identified whose GOF enhanced that of *jing*. This group of genes specifically interacts with *jing* and each other during ommatidial formation. Of these, we identified the Drosophila homolog of the disease gene of human α-thalassemia/mental retardation (MR) X-linked (*DATR-X*) (Gibbons *et al.* 1995b). The human ATR-X gene encodes a zinc-finger ATPase that is involved in chromatin remodeling and is the disease gene of several MR syndromes (Gibbons *et al.* 1995b; Villard *et al.* 1996a,b; Abidi *et al.* 1999; Xue *et al.* 2003; Tang *et al.*, 2004).

To explore the transcriptional mechanisms controlling axon patterning, we investigated the cell-specific roles of *jing* and *DATR-X* in regulating axon formation in the embryonic CNS. The roles of *DATR-X* and *jing* in the CNS were studied by reducing their expression specifically in neurons or glia using RNA interference (RNAi) and by analyzing the GOF effects of each gene. We show that *jing* and *DATR-X* have (1) autonomous roles in CNS glial survival, (2) autonomous and nonautonomous roles in LG and axon positioning, and (3) autonomous and nonautonomous roles in longitudinal axon outgrowth. The phenotypes of *jing* and *DATR-X* mutations derive from a perturbation in the extensive neuronal–glial communication mechanisms that govern CNS axon scaffold formation. Early ubiquitous expression of *DATR-X* mRNA and an enrichment of transcripts and reporter gene expression in embryonic neurons and glia reveal a similarity to the expression pattern of *jing* (Sedaghat *et al.* 2002). The combined effects of *jing* and *DATR-X* knockdown and GOF are synergistic and the phenotypes resulting from single gene knockdown are similar, providing strong evidence that *jing* and *DATR-X* may work together. Therefore, *jing* and *DATR-X* function is instrumental in the neuronal–glial communication mechanisms that govern CNS axon scaffold formation.

MATERIALS AND METHODS

Drosophila strains: All flies were raised on standard Drosophila cornmeal medium at 25° (Ashburner 1989). The collection of third chromosome transgenic EP strains, generated and described by Rørth (1996), was obtained from the Hungarian Szeged stock center. *GMR-Gal4* (second chromosome) was obtained from J. Nambu (Hay *et al.* 1994; Wing *et al.* 2002) and *paired* (*prd*)-*Gal4* (third chromosome) were obtained from S. Crews. The driver, *ELAV-Gal4* (on X), was used to drive expression in neurons and is a promoter fusion of the embryonic lethal abnormal vision gene (Robinow and White 1988; Yao and White 1994); it was obtained from the Bloomington stock center. *GCM-Gal4* drives expression in all CNS glia expressing the *glial cells missing* (*GCM*) gene and was obtained from M. Freeman (Freeman *et al.* 2003; Hosoya *et al.* 1995; Jones *et al.* 1995;). *btl-Gal4* was used to drive expression in the trachea (Shiga *et al.* 1996).

UAS-jingE, *jing* EMS alleles, and the *jing* deficiency [Df (2R)ST1] were previously described (Sedaghat *et al.* 2002; Sonnenfeld *et al.* 2004). *UAS-jing*U is a second chromosome insertion that expresses *jing* as determined by *in situ* hybridization.

Genetic crosses: Balancers were detected using Cyo *wingless-lacZ* or TM3 *ubx-lacZ*. *DATR-X* and *jing* were overexpressed in CNS neurons by crossing homozygous *ELAV-Gal4* with homozygous *UAS-jingE*, EP(3)0635, or *UAS-DATR-X*. For coexpression experiments, flies carrying *ELAV-Gal4* and *UAS-jingE* were crossed with flies homozygous for EP(3)0635. Controls included *ELAV-Gal4/+*, *UAS-jingE/+*, and EP(3)0635/+. For

double RNAi flies carrying *ELAV-Gal4* and UAS-*jing* RNAi were crossed to flies carrying UAS-*DATR-X* RNAi.

EP screen: Males from each EP line were crossed to virgin females carrying *GMR-Gal4*. The eye morphologies of F_1 male progeny from this cross were analyzed under a dissecting microscope and male flies with straight wings were then crossed to virgin females carrying *UAS-jingE*. One copy of *UAS-jingE* is not associated with a rough eye phenotype and therefore any rough eye phenotype in combination with a particular EP line and *GMR-Gal4* represented an interaction. The number of flies with rough eyes was determined under a dissecting microscope where at least 600 progeny were analyzed in each of three trials at 25°. Controls included in each trial included *GMR-Gal4/UAS-jingE* and *GMR-Gal4/+* and did not show a rough eye at 25°. As an additional control, eyes were inspected from flies heterozygous for *UAS-jingE* and the enhancing EP line. Enhancing lines were subjected to three more genetic trials with *GMR-Gal4* and *UAS-jingE* at 25°. The penetrance was determined as the number of rough eyes divided by the 25% that carried *GMR-Gal4*, *UAS-jingE*, and the particular EP strain. A total of 591 individual third chromosome EP lines were screened. Enhancer EP lines were tested for interactions *inter se* and with additional EP lines expressing DNA regulatory genes and random EP lines by the same method as described above.

Microscopy: For scanning electron microscopy (SEM), 1- to 3-day-old adult heads were dissected, fixed, and dehydrated by 15-min incubations in a graded ethanol series. Dehydrated heads were sent to the Mount Sinai Bioimaging Center (Toronto) for sputter coating with gold-palladium and SEM examination. Three eyes from each sample were examined and processed using Adobe Photoshop software. For light microscopy, 1- to 3-day-old adult heads were dissected, analyzed on a Zeiss Axioskop, and images were captured on a Nikon DXM1200 digital camera and processed using Adobe Photoshop software. Confocal microscopy was carried out on a BioRad1024 microscope using ×40 water immersion [1.15 numerical aperture (NA)] or ×20 (1.1 NA) objectives.

Antibodies and immunostaining of Drosophila embryos: The following antibodies were obtained from the Developmental Studies Hybridoma Bank (Iowa City, IA): BP102 (1:10), anti-Repo (8D12, 1:10) (Campbell *et al.* 1994), 1D4 (Fasciclin II, 1:10) (Van Vactor *et al.* 1993), and anti-Robo (13C9, 1:10) (Kidd *et al.* 1998a). A rabbit antibody against β-galactosidase (Promega) was used at 1:100 dilution. HRP-conjugated goat anti-mouse IgG was used at 1:100. Texas red and FITC-conjugated secondary antibodies were used for confocal microscopy. Monoclonal antibody 2A12 was used to visualize tracheal tubules (1:3).

Embryos were fixed in PBS containing 4% formaldehyde and embryos were incubated overnight with primary antibodies in PTN (1× PBS, 0.1% Triton X-100, 5% normal goat serum). Horseradish peroxidase-conjugated secondary antibodies were used with H_2O_2/diaminobenzedine histochemistry. Stained embryos were dehydrated through an ethanol series, mounted in methyl salicylate, and examined by Nomarski optics on a Zeiss Axioskop microscope. Images were captured on a Nikon DXM1200 digital camera and processed using Adobe Photoshop software.

Molecular genetic analysis of *DATR-X* and generation of *UAS* lines: Genomic and cDNA sequences encoding the Drosophila *DATR-X* homolog were identified by searching the Berkeley Drosophila Genome Project (BDGP) database for the EP(3)0635 associated gene (Adams *et al.* 2000; Rubin *et al.* 2000). The location of the EP element in EP(3)0635 was confirmed by PCR using inverted repeat primers and flanking genomic *DATR-X* sequence (CGACGGGACCACCTTATGTTATTTCATCATG) followed by DNA sequence analysis. *DATR-X* cDNAs [expressed sequence tags (ESTs) SD07188 and LD28477] were obtained from Open Biosystems and *jing* cDNA was previously obtained from Research Genetics (Sedaghat *et al.* 2002). *DATR-X* EST SD07188 contains 2382 bp of *DATR-X* coding sequence beginning at base pair 1968 with respect to full-length LD28477 cDNA sequence. *DATR-X* clones SD07188 and LD28477 were subjected to DNA sequence analysis and compared to that in the Gadfly database (Celera genomics) (Adams *et al.* 2000). Homology searches were done using BLAST (http://www.ncbi.nlm.nih.gov). Full-length *DATR-X* sequence (accession AAL13821; FlyBase) was aligned with that of *Caenorhabditis elegans* (AAD55361), mouse (AAC08741), and human (AAB49970) using Clustal X (1.83). Protein sequences were compared using BL2SEQ (http://www.ncbi.nlm.nih.gov/blast/bl2seq/wblast2.cgi) (Tatusova and Madden 1999). Protein domains were analyzed using SMART and PROSITE (Hulo *et al.* 2004; Letunic *et al.* 2004).

Full length *DATR-X* cDNA (LD28477) was subcloned into the pUAST vector (Brand and Perrimon 1993) as an *Eco*RI–*Kpn*I fragment and used to generate germline transformant flies by standard procedures (Genetic Services, Cambridge, MA) (Rubin and Spradling 1983). Expression of *DATR-X* was confirmed in multiple lines by *in situ* hybridization on embryos expressing different *DATR-X* upstream activating sequence transgenes under control of the *prd* gene transactivator (*prd-GAL4*).

***In situ* hybridization and reporter gene construction:** Whole-mount *in situ* hybridization was carried out using digoxigenin-labeled RNA probes according to Janody *et al.* (2000). The *DATR-X* riboprobe was generated by linearizing the SD07188 EST with *Hae*II. Sense probes were synthesized using the T7 promoter and antisense using Sp6 according to manufacturers' specifications (Roche). Probe specificity was tested in GOF *DATR-X* embryos carrying the *prd-Gal4* driver and EP(3)0635 or *UAS-DATR-X* transgenes. Third instar larval nerve cords were dissected in PBS and fixed in 4% formaldehyde for 20 min. Fixed nerve cords were rinsed three times in fresh PBS and washed for 1 hr. Nerve cords were then subjected to *in situ* hybridization as described above. Digoxigenin-stained nerve cords and embryos were mounted in 80% glycerol and examined on a Zeiss Axioskop 2.

A total of 1553 bp from the 5′ region of *jing* were obtained by PCR using Drosophila w^{1118} genomic DNA as template, sequenced, and cloned into the *Kpn*I and NotI sites of the pCaSper vector for *in vivo* expression. A total of 593 bp were obtained by PCR from the 5′ *DATR-X* region surrounding the EP element insertion site. This fragment was cloned into the *Eco*RI site in pCaSper. To generate transgenic strains, the pCaSper plasmids were co-injected together with a plasmid encoding Δ2-3 transposase into w^{1118} embryos by *P*-element-mediated transformation (Genetic Services) (Rubin and Spradling 1983). Multiple strains were analyzed for *lacZ* expression.

RNA interference: For *DATR-X* RNAi, a 697-bp sequence was generated by PCR from base pair positions 3181–3837 using LD28477 cDNA as a template. For RNAi of *jing*, a 597-bp sequence was generated by PCR from base pair position 2289 from the ATG on the LD36562 cDNA. The DNA fragments were individually subcloned sequentially, in opposite directions, into the *Avr*II and *Nhe*I sites of the pWIZ plasmid (a gift of R. Carthew) except that the inverted sequence was directionally cloned using *Xba*I and *Nhe*I restriction enzymes (Lee and Carthew 2003). The final inverted repeat containing vectors *UAS-DATR-X* RNAi and *UAS-jing* RNAi was confirmed by sequence analysis. To generate transgenic strains, the *UAS-DATR-X* RNAi or *UAS-jing* RNAi plasmids, were co-injected together with a plasmid encoding Δ2-3 transposase into w^{1118} embryos by *P*-element-mediated transformation (Genetic Services) (Rubin and Spradling 1983).

Several independent *UAS-DATR-X* RNAi and *UAS-jing* RNAi transformant lines were bred to homozygosity, mapped, and tested for double-stranded RNAi activity by crossing to CNS- (*ELAV-Gal4*) and tracheal-specific *Gal4* (*btl-Gal4*) drivers and immunostaining with monoclonal antibodies 1D4 and 2A12, respectively. To confirm downregulation of mRNA expression, embryos carrying *armadillo-Gal4* (Ahmad and Henikoff 2001) and *UAS-DATR-X* RNAi or *UAS-jing* RNAi were subjected to *in situ* hybridization using *DATR-X* or *jing* riboprobes, respectively. The number of stage 13 embryos with reduced expression in transgene- and *Gal4* driver-carrying embryos was compared with that in control embryos carrying either the driver or the transgene alone.

Quantitative analysis of longitudinal axon and glial cell defects: The number of crossovers per segment was counted in stage 16/17 control embryos and those expressing multiple *jing* or *DATR-X* RNAi transgenes were driven either by *ELAV-Gal4* or by *GCM-Gal4* and stained with 1D4 and anti-Robo. Four independent transgenic lines and controls were analyzed. Neuronal expression of pWiz-*DATR-X*022, pWiz-*DATR-X*28-MO1, pWiz-*DATR-X*26-MO2, and pWiz-*DATR-X*28-MO2 resulted in 20.9% ($n = 200$), 22% ($n = 178$), 27% ($n = 187$), and 30% ($n = 145$) of embryos with axon defects, respectively. Neuronal expression of pWiz-*jing*NC1A, pWiz-*jing*ORO3, pWiz-*jing*NA2, pWiz-*jing*006 resulted in 25% ($n = 180$), 29% ($n = 210$), 28% ($n = 168$), and 31% ($n = 201$) of embryos with axon defects, respectively.

Quantitative analysis of glia was carried out by light microscopy on anti-Repo stained whole-mount embryos from stage 11 to 16. Glia were counted in each nerve cord segment of embryos expressing four independent *jing* or *DATR-X* RNAi transgenes as driven either by *ELAV-Gal4* or by *GCM-Gal4*. Controls included embryos heterozygous for each RNAi transgene, the Gal4 driver as well as w^{1118}. Standard deviations in glial numbers in each sample were determined using Microsoft Excel and sample sizes exceeded 250 nerve cord segments. Differences in the number of glia in each sample relative to controls were evaluated for significance using Student's paired *t*-test. Any space in the longitudinal connectives was considered a longitudinal break.

RESULTS

Identification of the Drosophila homolog of human *ATR-X* and additional genes involved in *jing* function: Our approach to identify genes interacting with *jing* was to use the EP collection of strains including genes tagged by insertion of a transposable element containing *UAS* sites (Szeged stock center, Szeged, Hungary) (Brand and Perrimon 1993; Rørth 1996). We reasoned that *jing* GOF may show dosage effects in the larval eye that could be easily scored in the adult since this neural tissue is sensitive to studies of transcriptional regulatory mechanisms (Rubin 1988; Zipursky and Rubin 1994) and *jing* has a neuronal function (Sedaghat *et al.* 2002).

TABLE 1

EP lines that enhanced *jing* gain of function

EP line	Gene	Predicted function
EP(3)0635	*ATR-X/XNP*	Chromatin remodeling
EP(3)0473	*D1*	Chromatin remodeling
EP(3)3145	*Dataxin-2*	Translational regulation
EP(3)3060	*lap*	Receptor-mediated endocytosis
EP(3)3705	CG32137	Microtubule binding (cell cycle)
EP(3)3354	CG17383 (JIGR-1)	Transcriptional regulation
EP(3)3084	CG15507	Unknown

Rough eyed flies were scored in a population carrying *GMR-Gal4*, *UAS-jing*, and each EP line under a dissecting microscope. Crosses were repeated at least three times at 25° totaling a sample size of >1200 flies.

An enhancer screen was carried out using the third chromosome collection of EP lines (see materials and methods) (Rørth 1996). Of 591 third-chromosome EP lines screened, 7 were found to repeatedly interact genetically when coexpressed with *jing* in the eye under control of *GMR-Gal4* (Table 1; Figure 1). Eye-specific expression of one copy of a UAS-*jing* transgene has no visible effects on ommatidial formation (Figure 1B) as compared with eyes heterozygous for *GMR-Gal4* (Figure 1A). However, coexpression of *jing* with EP(3)0635, which controls expression of the Drosophila homolog of human ATR-X (*DATR-X*), disrupted ommatidial formation (Figure 1D). Eye-specific expression of EP(3)0635 alone had no effect (Figure 1C). *jing* also interacted with 4 other EP lines, including EP(3)3145, EP(3)3705, EP(3)3354, and EP(3)0473, resulting in rougher eyes (Figure 1, F, K–M). A loss in pigmentation occurred in the case of EP(3)3354. These lines had no effect when expressed alone in the eye (Figure 1N; Table 2).

Two additional EP lines that interacted with *jing* caused a rough eye phenotype when expressed alone in the eye, including EP(3)3084 (Figure 1G) and EP(3)3060 (Figure 1I). *GMR-Gal4*-driven expression of EP(3)3084 was associated with morphological defects, mild reductions in pigmentation, and glossy eyes in 100% of flies (Figure 1, G and N; Figure 2A). However, coexpression of EP(3)3084 with *jing* resulted in an enhancement of this phenotype in which eye size was reduced, eyes were rougher, and pigmentation was completely lost (Figure 1H; Figure 2B). A total of 35% of eyes with a phenotype were enhanced ($n = 345$).

Figure 1.—Identification of enhancer/promoter (EP) lines that enhance *jing* gain –of function in the eye. (A–M) Scanning electron micrographs of adult eyes of the following genotypes are shown: (A) *GMR-GAL4/+*; (B) *GMR-GAL4/+*; *UAS-jingE/+*; (C) *GMR-GAL4 /+*; EP(3)0635/+; (D) *GMR-GAL4/+*; *UAS-jingE /+*; EP(3)0635/+; (E) *GMR-GAL4/+*; EP(3)3145/+; (F) *GMR-GAL4/+*; *UAS-jingE /+*; EP(3)3145/+; (G) *GMR-GAL4/+*; EP(3)3084/+; (H) *GMR-GAL4/+*; *UAS-jingE /+*; EP(3)3084/+; (I) *GMR-GAL4/+*; EP(3)3060/+; (J) *GMR-GAL4/+*; *UAS-jingE /+*; EP(3)3060/+; (K) *GMR-GAL4/+*; EP(3)3705 /+; *UAS-jingE/+*; (L) *GMR-GAL4/+*; *UAS-jingE /+*; EP(3)3354/+; (M) *GMR-GAL4/+*; *UAS-jingE /+*; EP(3)0473/+. (N) Penetrance values of enhancing phenotypes. Bars, 100 μm.

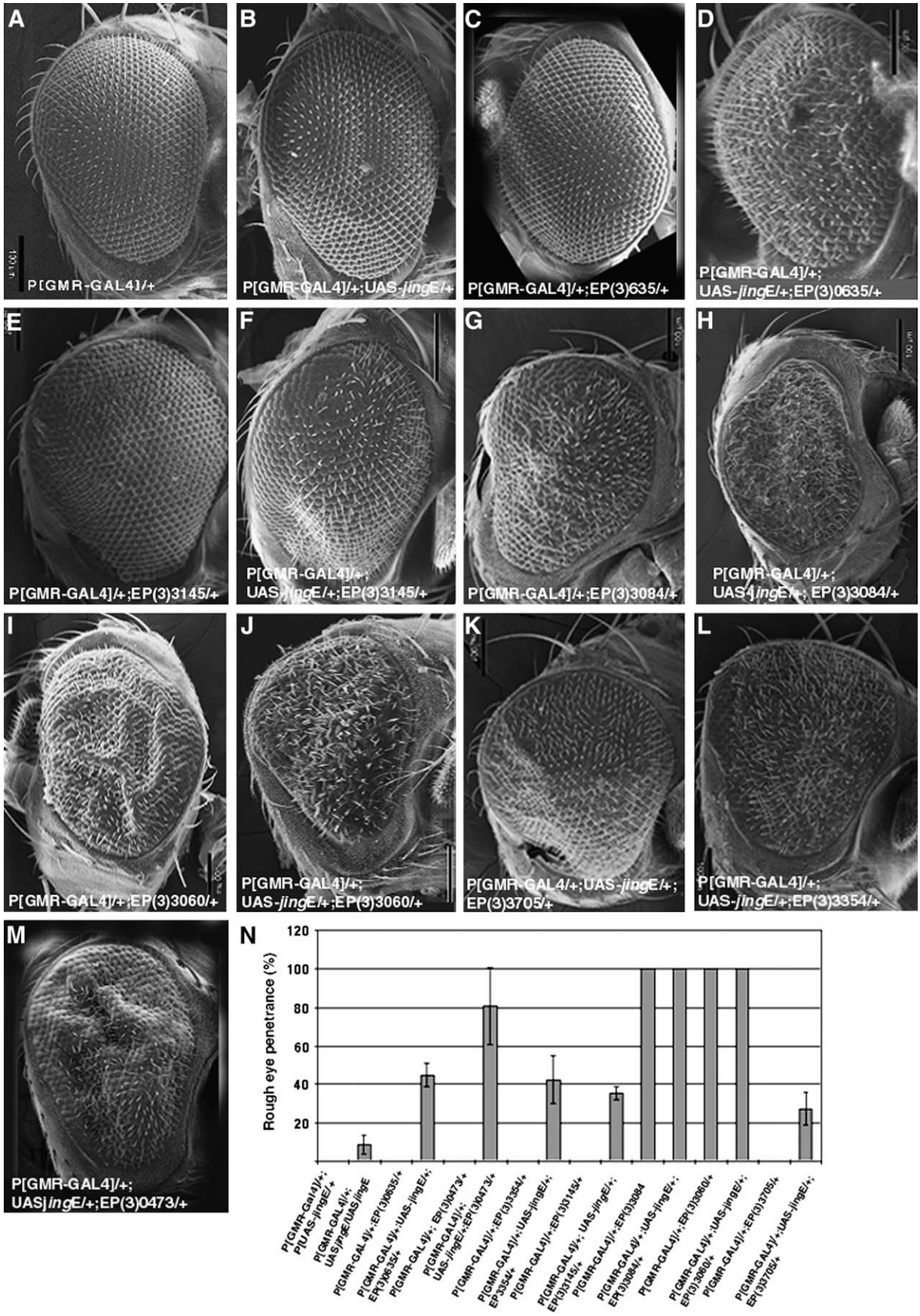
A
P[GMR-GAL4]/+
B
P[GMR-GAL4]/+;UAS-jingE/+
C
P[GMR-GAL4]/+;EP(3)635/+
D
P[GMR-GAL4]/+;
UAS-jingE/+;EP(3)0635/+
E
P[GMR-GAL4]/+;EP(3)3145/+
F
P[GMR-GAL4]/+;
UAS-jingE/+;EP(3)3145/+
G
P[GMR-GAL4]/+;EP(3)3084/+
H
P[GMR-GAL4]/+;
UAS-jingE/+; EP(3)3084/+
I
P[GMR-GAL4]/+;EP(3)3060/+
J
P[GMR-GAL4]/+;
UAS-jingE/+;EP(3)3060/+
K
P[GMR-GAL4/+;UAS-jingE/+;
EP(3)3705/+
L
P[GMR-GAL4]/+;
UAS-jingE/+;EP(3)3354/+
M
P[GMR-GAL4]/+;
UASjingE/+;EP(3)0473/+
N
Rough eye penetrance (%)
120
100
80
60
40
20
P[GMR-Gal4]/+;
P[UAS-jingE]/+
P[GMR-GAL4]/+;
UAS-jingE/UAS-jingE
P[GMR-GAL4]/+;EP(3)0635/+
P[GMR-GAL4]/+;UAS-jingE/+;
EP(3)0635/+
P[GMR-GAL4]/+; EP(3)0473/+
P[GMR-GAL4]/+;
UAS-jingE/+;EP(3)0473/+
P[GMR-GAL4]/+;EP(3)3354/+
P[GMR-GAL4]/+;UAS-jingE/+;
EP3354/+
P[GMR-GAL4]/+;EP(3)3145/+
P[GMR-GAL4]/+; UAS-jingE/+;
EP(3)3145/+
P[GMR-GAL4]/+;EP(3)3084
P[GMR-GAL4]/+;UAS-jingE/+;
EP(3)3084/+
P[GMR-GAL4]/+;EP(3)3060/+
P[GMR-GAL4]/+;UAS-jingE/+;
EP(3)3060/+
P[GMR-GAL4]/+;EP(3)3705/+
P[GMR-GAL4]/+;UAS-jingE/+;
EP(3)3705/+

TABLE 2

Random screening of *jing* interacting EP lines

	Eye phenotype	Sample size		Eye phenotype	Sample size
P[*GMR-Gal4*] ×			P[*GMR-Gal4*]-EP(3)0473 ×		
EP(3)3339	Wild type	250	EP(3)3339	Rough	200 (60)
EP(3)3303	Wild type	178	EP(3)3303	Rough	250 (40)
EP(3)3258	Wild type	189	EP(3)3258	Rough	214 (37)
EP(3)3916	Wild type	201	EP(3)3916	Rough	210 (23)
EP(3)893	Wild type	200	EP(3)893	Rough	276 (16)
EP(3)3377	Wild type	215	EP(3)3377	Rough	234 (42)
P[*GMR-Gal4*]-EP(3)3084 ×	Glossy, ↓pigment	400	P[*GMR-Gal4*]-EP(3)3060 ×	Rough	450
EP(3)3339	No change	260	EP(3)3339	Enhanced	76 (20)
EP(3)3303	No change	201	EP(3)3303	Enhanced	60 (53.3)
EP(3)3258	No change	192	EP(3)3258	Enhanced	60 (6.7)
EP(3)3916	No change	189	EP(3)3916	No change	150
EP(3)893	No change	234	EP(3)893	No change	200
EP(3)3377	No change	250	EP(3)3377	Enhanced	160 (75)
P[*GMR-Gal4*]; EP(3)0635 ×	Wild type	650	P[*GMR-Gal4*]; EP(3)3145 ×	Wild type	630
EP(3)3339	Wild type	251	EP(3)3339	Wild type	151
EP(3)3303	Wild type	234	EP(3)3303	Wild type	145
EP(3)3258	Wild type	243	EP(3)3258	Wild type	130
EP(3)3916	Wild type	267	EP(3)3916	Wild type	125
EP(3)893	Wild type	154	EP(3)893	Mild rough	218 (6.4)
EP(3)3377	Wild type	134	EP(3)3377	Wild type	245
P[*GMR-Gal4*]; EP(3)3354 ×	Wild type	550	P[*GMR-Gal4*]; EP(3)3705 ×	Wild type	601
EP(3)3339	Wild type	200	EP(3)3339	Wild type	160
EP(3)3303	Wild type	250	EP(3)3303	Wild type	134
EP(3)3258	Wild type	214	EP(3)3258	Wild type	191
EP(3)3916	Wild type	210	EP(3)3916	Wild type	230
EP(3)893	Wild type	276	EP(3)893	Wild type	212
EP(3)3377	Wild type	234	EP(3)3377	Wild type	213

Sample sizes include the total number of progeny. Sample sizes for EP lines with a phenotype, such as EP(3)3060, EP(3)3084, and EP(3)0473, include the number of eyes with a phenotype. Percentages in parentheses indicate the penetrance as the number of enhanced eyes over the total number of eyes with a phenotype.

Eye-specific expression of EP(3)3060 caused a mild rough eye (Figure 1I) with no loss in pigmentation (Figure 2G). Enhancement of this phenotype was observed after EP(3)3060 and *jing* coexpression, which included rougher eyes (Figure 1J) and loss in pigmentation (Figure 2H). A total of 38% of eyes with a phenotype were enhanced ($n = 301$).

Specificity of EP interactions: The genetic synergy between *jing* and the enhancers suggests that these genes may function in similar processes in neural cells. However, the group of *jing*-interacting genes are involved in a wide range of functions, including chromatin remodeling (*DATR-X* and *D1*) (Rodriguez-Alfageme *et al.* 1980; Ashley *et al.* 1989; Gibbons *et al.* 1995b; Picketts *et al.* 1996), transcriptional regulation [EP(3) 3354] (Ewel *et al.* 1990; England *et al.* 1992; Cutler *et al.* 1998; Brody *et al.* 2002; Bhaskar and Courey 2002), translational regulation [EP(3)3145, *Datx2*] (Satterfield *et al.* 2002; Ciosk *et al.* 2004), synaptic vesicle transport [EP(3)3060] (Pena-Rangel *et al.* 2002), and cell cycle control [EP(3)3705] (BDGP). To test the specificity of the interactions with *jing*, the enhancers were crossed with six random EP lines, including EP(3) 3339, EP(3)3303, EP(3)3258, EP(3)3916, EP(3)893, and EP(3)3377, and were driven in the eye with *GMR-Gal4*. Of the enhancers, only EP(3)3060 and EP(3)0473 interacted with multiple EP lines (Table 2; Figure 2, I and J). In addition, EP(3)3145 interacted with EP(3)0893, resulting in mildly rough eyes (Table 2).

Next, we addressed the specificity of *D1* and *DATR-X* enhancement by testing for interactions with other regulatory genes in the EP collection. *DATR-X* [EP(3)635] did not interact with other EP elements upstream from genes encoding DNA-binding proteins, including

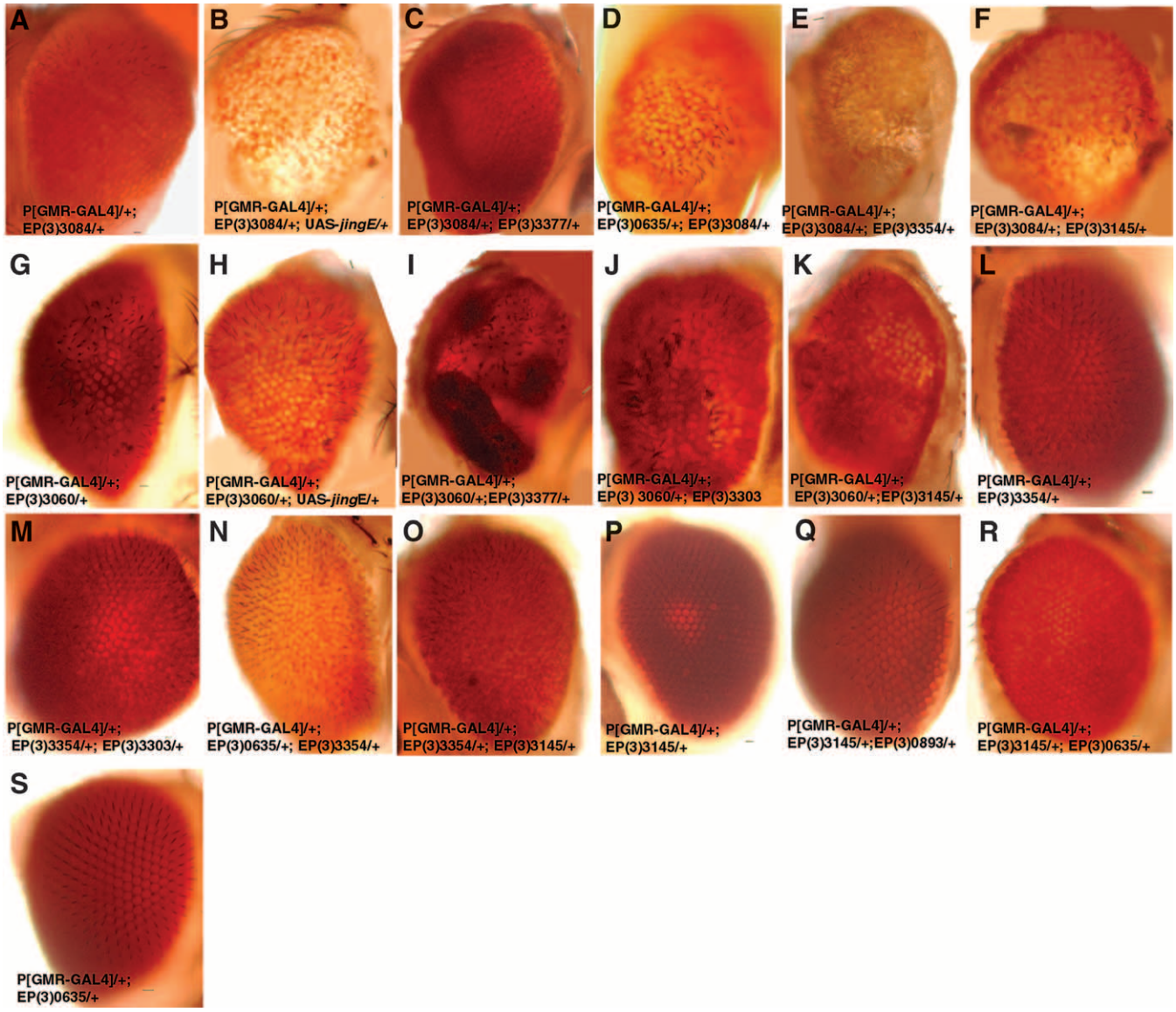

Figure 2.—Genetic interactions of *jing* enhancers. Light level images of adult eyes of the following genotypes are shown: (A) *GMR-GAL4* /+; EP(3)3084/+; (B) *GMR-GAL4*/+; EP(3)3084/+; UAS-*jingE*/+; (C) *GMR-GAL4*/+; EP(3)3084/+; (D) EP(3)3377/+; *GMR-GAL4*/+; EP(3)0635/+; EP(3)3084/+; (E) *GMR-GAL4*/+; EP(3)3084/+; EP(3)3354/+; (F) *GMR-GAL4*/+; EP(3)3084/+; EP(3)3145/+; (G) *GMR-GAL4*/+; EP(3)3060/+; (H) *GMR-GAL4*/+; EP(3)3060/+; UAS-*jingE*/+; (I) *GMR-GAL4*/+; EP(3)3060/+; EP(3)3377/+; (J) *GMR-GAL4*/+; EP(3)3060/+; EP(3)3303/+; (K) *GMR-GAL4*/+; EP(3)3060/+; EP(3)3145/+; (L) *GMR-GAL4*/+; EP(3)3354/+; (M) *GMR-GAL4*/+; EP(3)3354/+; EP(3)3303/+; (N) *GMR-GAL4*/+; EP(3)0635/+; EP(3)3354/+; (O) *GMR-GAL4*/+; EP(3)3354/+; EP(3)3145/+; (P) *GMR-GAL4*/+; EP(3)3145/+; (Q) *GMR-GAL4*/+; EP(3)3145/+; EP(3)0893/+; (R) *GMR-GAL4*/+; EP(3)3145/+; EP(3)0635/+; (S) *GMR-GAL4*/+; EP(3)0635/+. Bars, 50 μm.

EP(3)1005 ($n = 411$) and EP(3)1096 ($n = 387$). The *P* element in line EP(3)1005 lies upstream from CG15514, which encodes a protein containing a DNA-binding BED finger found in chromatin-boundary-element-binding proteins and transposases (FlyBase) (Aravind 2000). The *P* element in line EP(3)1096 lies upstream of a gene encoding a CXXC zinc finger (FlyBase, CG11033). EP(3)0635 did not interact with EP(3)3058 ($n = 200$), which lies upstream from the *poly U binding factor 68kD* (*pUf68*) gene (Page-McCaw *et al.* 1999; Lasko 2000). However, EP(3)0635 did interact with EP(3)3205 (35% penetrance, $n = 301$), which lies upstream of CG7552 encoding a protein with a WW domain and interacts genetically with cyclin E (Tseng and Hariharan 2002). In contrast, EP(3)0473 interacted with EP(3)1005 (48%, $n = 205$), EP(3)3205 (12%, $n = 150$), and EP(3)3058 (83%, $n = 256$), indicating that it may be a more general transcriptional regulator.

Interenhancer interactions: Last, we determined if the *jing* enhancers interacted with each other in the eye. Eye-specific coexpression of EP(3)3084 with EP(3)0635, EP(3)3354, and EP(3)3145 resulted in more severe

TABLE 3

Screening of *jing* interacting EP lines

P[*GMR-Gal4*]; EP(3)3145	Eye phenotype	% penetrance	*N*	P[*GMR-Gal4*]; EP(3)0635	Eye phenotype	% penetrance	*N*
EP(3)0635	Glossy, ↓↓ pigment	17.9	217	EP(3)3084	↓↓↓ pigment	46.1[a]	256
EP(3)3060	Bumpy, ↓ pigment	49.0[a]	300	EP(3)3354	Glossy, ↓↓↓ pigment	17.2	93
EP(3)3354	Glossy, ↓↓ pigment	14.1	85	EP(3)3060	Glossy, ↓↓ pigment	88.9[a]	90
EP(3)3084	Rougher, ↓↓↓ pigment	30.8[a]	65	EP(3)3705	Rough	20	200
EP(3)3705	Rough	8.5	94	EP(3)0473	Rough	18.8	223
EP(3)0473	Rough	15.0	167				

P[*GMR-Gal4*]; EP(3)3084	Eye phenotype	% penetrance	*N*	P[*GMR-Gal4*]; EP(3)3060	Eye phenotype	% penetrance	*N*
EP(3)3060	No change	0	250	EP(3)3354	Smaller, rougher	40[a]	70
EP(3)3354	Glossy, ↓↓↓ pigment	21.4[a]	234	EP(3)473	Rougher	7.5[a]	90
EP(3)0473	Rougher	24.9[a]	201	EP(3)3705	Smaller, rougher	18.7[a]	75
EP(3)3705	Rougher	20.8[a]	120				

P[*GMR-Gal4*]; EP(3)3354	Eye phenotype	% penetrance	*N*
EP(3)3705	Small	18.4	250
EP(3)0473	Rough	15.6	225

Penetrance is indicated by percentage of the eyes with a phenotype out of the progeny carrying *GMR-Gal4* and the EP elements. *N*, sample sizes.

[a] Penetrance for EP lines with a phenotype such as EP(3)3060, EP(3)3084, and EP(3)0473 is the percentage of the enhanced eyes out of the total eyes with a phenotype.

rough eye phenotypes including losses in pigmentation (Figure 2, D–F; Table 3). Eye-specific expression of EP(3)3060 resulted in rougher eyes when coexpressed with EP(3)3145, EP(3)3354, EP(3)0635, EP(3)0473, and EP(3)3705 (Figure 2K; Table 3). However, the widespread interactions of EP(3)3060 suggest that these results may be considered nonspecific (Table 2; Figure 2, I and J).

Eye-specific coexpression of EP(3)3354 with EP(3)3145 and EP(3)0635 resulted in glossy eyes with severely reduced pigmentation representing synergistic interactions (Table 3; Figure 2, N and O). We have designated EP(3)3354 as ***j**ing* **i**nteracting **g**ene **r**egulatory **1** (JIGR1), given its potential role in regulating gene expression (Brody *et al.* 2002). The EP element in *JIGR1* lies upstream of the transcript CG17383, which was identified in a differential head cDNA screen (Brody *et al.* 2002). JIGR1 contains an MADF domain shown in the Adf-1 transcription activator to bind DNA specifically to several developmentally regulated Drosophila gene promoters (Ewel *et al.* 1990; England *et al.* 1992; Cutler *et al.* 1998; Bhaskar and Courey 2002). *JIGR1* also interacted with EP(3)3705 resulting in a reduced eye size (Table 3).

EP(3)3145 lies upstream of *Drosophila ataxin2* (*Datx2*) and interacted with other *jing* enhancers from the screen but not with most randomly chosen EP lines. We observed glossy eyes and reduced pigmentation after coexpression of EP(3)3145 with EP(3)635 and EP(3)3354 (Figure 2, R and O). Collectively, these results identify a group of genes that have related functions pertaining specifically to *jing* and each other during eye development.

Part of ATR-X is highly conserved: Previous studies showed that ATR-X is involved in gene regulation by chromatin remodeling functions (Cardoso *et al.* 1998; Xue *et al.* 2003; Tang *et al.* 2004). Given the GOF interactions between *DATR-X* and *jing* in the eye, we proposed that there may be a regulatory relationship between DATR-X and Jing in the embryonic CNS and initiated further studies of *DATR-X*. Database searches with genomic sequence flanking the EP(3)0635 *P* element confirmed that the transposon in the strain we had obtained was inserted in the 5′-untranslated region of the predicted gene CG4548 encoding the Drosophila homolog of human *XNP/DATR-X* (GadFly).

DATR-X is located at cytological interval 96E1 on the third chromosome (BDGP) and encodes a predicted polypeptide of 1311 amino acids with 49.4% overall similarity to that of human ATR-X by alignment using the Clustal X algorithm (Figure 3A). *ATR-X* homologs are found in human, mouse, *C. elegans*, planarians, and Drosophila (Figure 3, A and C) (Villard *et al.* 1999). Most of the sequence conservation between human and *DATR-X* is confined to the helicase and SNF2 domains. The SNF2 domains of *C. elegans*, mouse, and human ATR-X show 54.9, 66.4, and 65.8% amino acid identity with that of *DATR-X*,

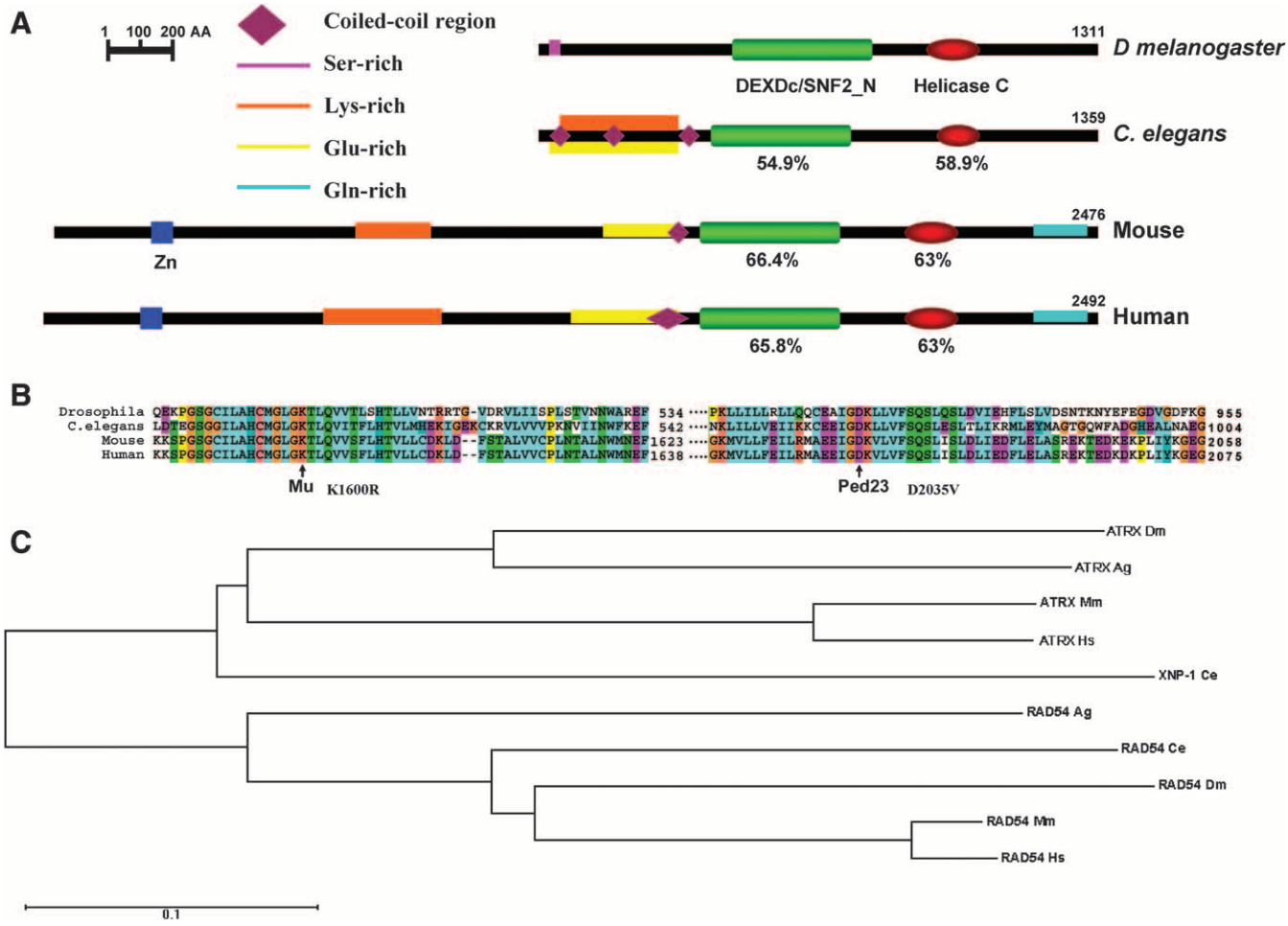

FIGURE 3.—ATR-X homologs. (A) Comparison of *DATR-X* protein domain architecture as predicted using SMART and PROSITE. Invertebrate ATR-X is truncated in comparison with mouse and human but shares high identities in the C-terminal amino acids with the latter proteins. Percentage of identity between the SNF2 and helicase C domains of *C. elegans*, mouse, and human are in comparison to those of *D. melanogaster*. (B) Comparison of amino acid identity over the regions containing mutations found in the ATPase domain of ATR-X from human patients with ATR-X syndrome. The mutations include both Mu K1600R and Ped23 D2035V in highly conserved regions. (C) Phylogenetic analysis of ATR-X orthologs. The distance between any two sequences is the sum of horizontal branch length separating them. Sequences were aligned using CLUSTALW (Tree View). The sequence residues in each column are colored on the basis of an alignment consensus, which is calculated automatically (for detail color information, refer to CLUSTAL W online help). Species designation follows each protein acronym (Dm, *Drosophila melanogaster*; Ag, *Anopheles gambiae*; Mm, murine; Hs, human; Ce, *Caenorhabditis elegans*). Bar indicates the number of substitutions.

respectively (Figure 3A). The ATPase domains of *C. elegans*, mouse, and human ATR-X show 58.9, 63, and 63% amino acid identity with that of *DATR-X*, respectively (Figure 3A). ATR-X has nucleosome-stimulated ATPase activity that is used to modify chromatin structure and that is a common site of patient mutations (GIBBONS *et al.* 1995b; XUE *et al.* 2003; TANG *et al.* 2004). Mutations associated with MR are in invariant residues and the amino acids at the sites of two human mutations, designated Mu K1600R and Ped23 D2035V, are conserved in *DATR-X* (Figure 3B).

There are some differences in the amino acid sequences of vertebrate and invertebrate ATR-X. Human and mouse ATR-X have a zinc-finger DNA-binding domain consisting of three multicysteine zinc-finger motifs (C_2-C_2) that is not present in invertebrate ATR-X proteins (Figure 3A) (CARDOSO *et al.* 2000). These zinc fingers are required for nuclear localization and DNA binding by ATR-X (CARDOSO *et al.* 2000). Therefore, it is possible that invertebrate ATR-X proteins require site-specific DNA targeting to carry out their ATPase activities. The C terminal of ATR-X has a region rich in poly glutamine repeats (Figure 3A) proposed to be involved in protein–protein interactions that also is not present in either *D. melanogaster* or *C. elegans* ATR-X (PICKETTS *et al.* 1996; data not shown). Sequence distances between *ATR-X* orthologs in different species are schematized in Figure 3C.

***DATR-X* and *jing-lacZ* are expressed in CNS glia and neurons:** To determine the expression pattern of *DATR-X* during development, we hybridized whole-mount control embryos with digoxigenin-labeled antisense

and sense *DATR-X* riboprobes. Ectopic activation of EP(3)0635 was detected in *prd*-expressing stripes with our antisense *DATR-X* probe confirming the specificity of the probe and EP line (Figure 4A). *DATR-X* transcripts are present at a low level throughout cellular blastoderm embryos (Figure 4B) and during gastrulation (Figure 4C). In stage 15 embryos, *DATR-X* transcripts become enriched in the neuroectoderm and supraesophageal ganglion (brain) (Figure 4, D and G). In the mature ventral nerve cord, *DATR-X* mRNA is expressed in cells along the position of the longitudinal axon tracts (Figure 4G, arrows) and in more laterally located glia (Figure 4G, arrowhead). Similar CNS expression patterns were not observed in embryos hybridized with sense *DATR-X* riboprobes (Figure 4F). *DATR-X* transcripts are also present throughout the brains of third instar wild-type larvae but are predominant in the optic lobe region (Figure 4E).

To better understand the pattern of expression, we costained embryos carrying *jing*- and *DATR-X-lacZ* reporter genes with anti-β-galactosidase and the glial-specific anti-Repo antibody. Analysis by confocal microscopy revealed that *jing-lacZ* and *DATR-X-lacZ* are expressed in both glial and neuronal lineages. Many of the *DATR-X-lacZ*- and *jing-lacZ*-expressing glia are present in positions characteristic of the LG (Figure 4, I–R). Other *DATR-X-lacZ*- and *jing-lacZ*-expressing glia occupy more lateral (Figure 4, K and L, arrowheads) or ventral regions (Figure 4, N, O, S).

Pan-neural coexpression of *DATR-X* and *jing* synergistically disrupts longitudinal axon formation: Since coexpression of *jing* and *DATR-X* strongly affected adult neuronal development we wanted to determine if their coexpression had similar affects in embryonic neurons. *jing* and *DATR-X* were expressed in all postmitotic neurons with *ELAV*-GAL4. Expression of either *jing* or *DATR-X* alone resulted in subtle defects in the CNS axon scaffold as observed with BP102 staining. These defects included thinner longitudinal connectives (Figure 5, B and C, arrowheads) and reduced spacing between the anterior and posterior commissures (Figure 5, B and C, arrows). Additive effects were observed after expression of two copies of either *jing* (Figure 5E) or *DATR-X* (Figure 5F) where commissural axons were not properly separated (Figure 5, E and F, arrows).

Pan-neural coexpression of *jing* and *DATR-X* resulted in more severe defects in axonal patterning than expression of one or two copies of either transgene alone. An average of 65% of segments had no longitudinal connectives after *jing* and *DATR-X* coexpression (Figure 5D, arrowhead; Figure 5G) in comparison with expression of two copies of UAS-*jing* (5% of segments, $n = 80$) and EP(3)0635 (18% of segments, $n = 55$) (Figure 5G). Therefore, *jing* and *DATR-X* coexpression has synergistic effects specifically in embryonic CNS neurons.

Neuronal-specific functions of *jing* and *DATR-X* are required for repulsion of longitudinal axons and glia from the CNS midline: We targeted *DATR-X* and *jing* mutations to discern the neuronal and glial contributions of each gene product to axon scaffold formation. *DATR-X* and *jing* expression was knocked down using conditional RNAi (Hammond *et al.* 2001; Lee and Carthew 2003). A total of 697- and 567-bp sequences from nonconserved regions of *DATR-X* and *jing* were separately subcloned into a P[UAST] derivative plasmid to produce intron-spliced hairpin RNA corresponding to the *DATR-X* and *jing* genes, respectively. The *UAS/Gal4* system (Brand and Perrimon 1993) was then used to allow hairpin RNA to conditionally downregulate *DATR-X* and *jing* expression in specific cell lineages, which was confirmed by *in situ* hybridization. Penetrance values of CNS axon phenotypes associated with neuronal and glial knockdown of *jing* and *DATR-X* ranged from 24 to 30% (see materials and methods).

Longitudinal connective formation was analyzed in homozygous *jing* mutant embryos and those with neuronal-specific knockdown of *jing* and *DATR-X* stained with an antibody to Fasciclin II (1D4). Neuronal specificity was directed by the *ELAV-Gal4* driver. In these mutant embryos, FasII-positive longitudinal axons aberrantly cross the CNS midline in stage 16 embryos (Figure 6, B–D, arrowheads; Figure 6M). In addition, there are breaks in the longitudinal connectives suggesting axon outgrowth defects (Figure 6, C and D, arrows). In embryos with simultaneous neuronal knockdown of *jing* and *DATR-X* all FasII-positive lateral fascicles fuse into a single tract at the CNS midline (Figure 6E). These results establish an autonomous neuronal requirement for *jing* and *DATR-X* function in the outgrowth and lateral positioning of longitudinal axons and a genetic synergy during this process.

Consistent with these results, pan-neural knockdown of *jing* or *DATR-X* was associated with high levels of Robo at the CNS midline during both stage 12 (Figure 6, G

Figure 4.—Drosophila *ATR-X* and *jing* are expressed in CNS glia and neurons. *In situ* hybridization using a *DATR-X* digoxigenin-labeled riboprobe and showing wild-type whole-mount embryos with anterior to the left (A–G). Confocal micrographs of stage 15 whole-mount embryos (H–S). Embryos are stained with polyclonal rabbit anti-β-galactosidase (FITC-conjugated secondary antibody, green) and anti-Repo (Texas Red-conjugated secondary antibody, red). (A) To validate the probe specificity, an embryo ectopically expressing *DATR-X* in ectodermal stripes (arrow) of the *paired* gene was hybridized with a *DATR-X* riboprobe. The embryo carries *paired-GAL4* and EP(3)0635. (B) *DATR-X* transcripts are present in cellular blastoderm embryos. (C) A 5.5- to 6-hr-old embryo showing *DATR-X* transcripts in the supraesophageal ganglion (arrowhead) and neuroectoderm (arrow) in sagittal view. (D) A sagittal stage 15 embryo showing elevated *DATR-X* transcripts in the supraesophageal ganglion (arrowhead) and ventral nerve cord (arrow). (E) Third instar larval CNS expressing *DATR-X* in the brain hemispheres (arrow) and ventral ganglion

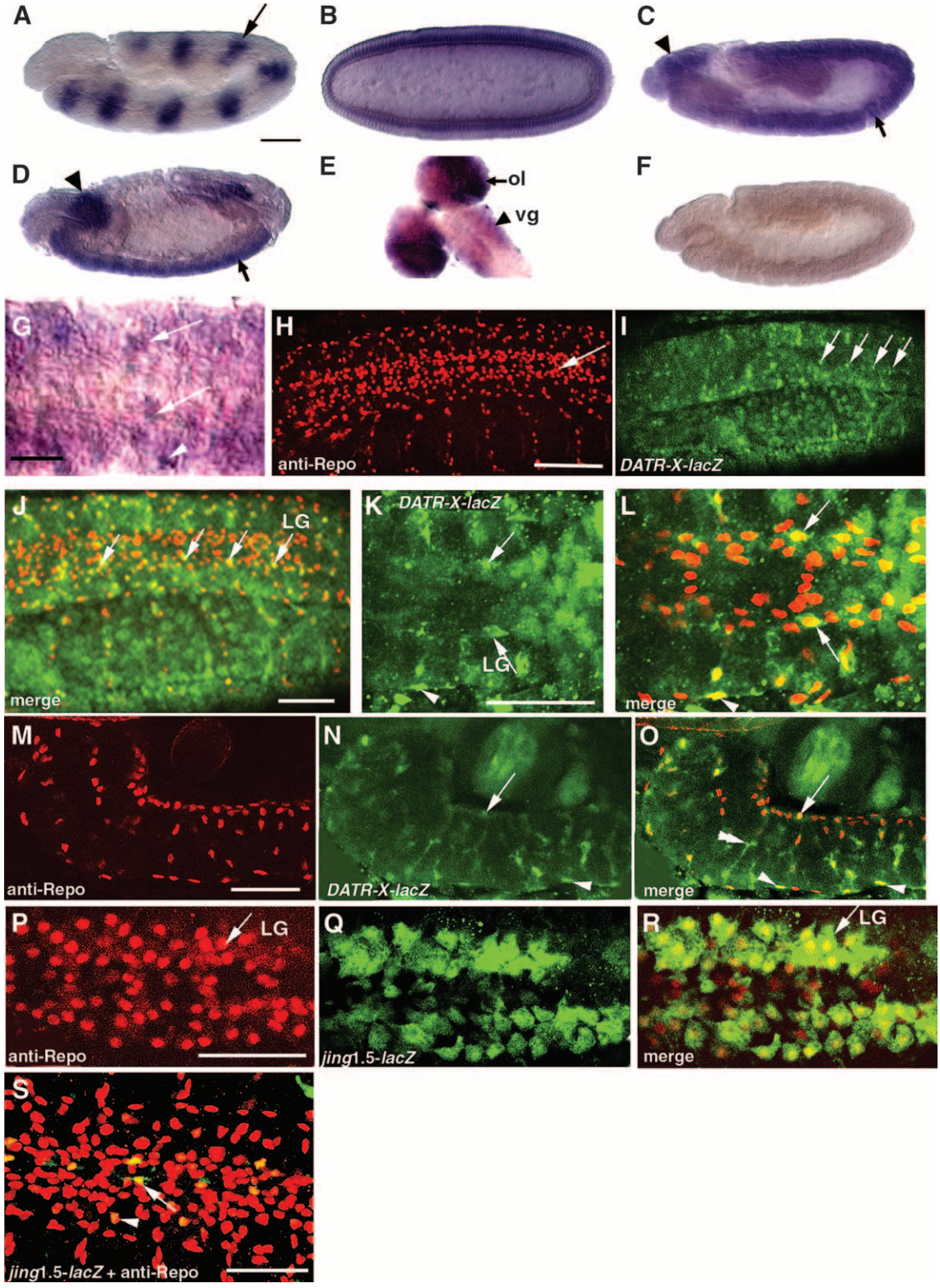

(arrowhead). *DATR-X* is expressed most strongly in the ventral region of the ganglion (vg, arrowhead) and optic lobe (ol, arrow). (F) *In situ* hybridization using a *DATR-X* negative control sense probe. (G) *DATR-X* expression in a stage 15 ventral nerve cord (ventral view). Strong expression is observed in cells lining the longitudinal connectives (arrows) and in lateral cells (arrowhead). (H–R) Focal planes of *DATR-X* and *jing-lacZ* expression in the longitudinal glia (LG) (arrows). (N and O) Sagittal views to show that *DATR-X-lacZ* is expressed in ventral glia (arrowhead) and the dorsal longitudinal glia (arrow). *DATR-X-lacZ* is also expressed in neurons (double arrowhead). (P–R) *jing-lacZ* is strongly expressed in the two rows of longitudinal glial cells. (S) *jing-lacZ* is also expressed in a bilateral glial lineage (arrow) and in a laterally located lineage (arrowhead) in the ventral focal plane. Bars: (A–F) 200 μm; (G) 30 μm; (H–S) 50 μm.

and H) and stage 16 (Figure 6, J and K). The phenotypes were variable (Figure 6K), as in the most severe case all Robo-positive axons were present at the midline (Figure 6K) and in less severe cases midline Robo was observed in fewer hemisegments (Figure 6L, arrowhead). We also observed breaks in Robo-positive connectives (Figure 6L, arrow). The high Robo levels in *jing* and *DATR-X* pan-neural mutants suggest that these genes do not regulate *robo* expression. However, the medial axon displacement suggests that these mutations may affect the expression of other genes required for Robo to read the Slit cue. Alternatively, *jing* and *DATR-X* may regulate longitudinal positioning in a Robo-independent manner (Kinrade *et al.*, 2001).

Glial functions of Jing and *DATR-X* are required for ipsilateral positioning of longitudinal glia, glial survival, and patterning of longitudinal axons: Genetic and cell ablation experiments have shown the critical role that neuronal–glial communication plays during pioneering of the longitudinal axon tracts (Booth *et al.* 2000; Hidalgo and Booth 2000; Hidalgo *et al.* 2001; Kinrade *et al.* 2001; Whitington *et al.* 2004). We therefore thought it might be informative to examine whether *jing* and *DATR-X* play a role in glial guidance of longitudinal axons. Glial development was examined after pan-glial expression of *jing* and *DATR-X* RNAi transgenes under the control of *glial cells missing* (*gcm*)-*Gal4* (Hosoya *et al.* 1995; Jones *et al.* 1995) and using anti-Repo as a marker to assess glial fates (Campbell *et al.* 1994; Xiong *et al.* 1994; Halter *et al.* 1995).

Robo-positive and Repo-positive LG were already misplaced medially during stage 12 after pan-glial knockdown of *jing* and *DATR-X* (Figure 7, C–F) and in *jing* hemizygotes (Figure 7B). Wild-type numbers of glia in these mutants at this stage reveal that *jing* and *DATR-X* are involved in glial differentiation and not in the division or specification of these cells (Figure 7O). Later during wild-type embryogenesis Robo is present only in axons (see Figure 6I) and therefore glial movement is restricted by Robo-independent mechanisms, including axon contact and trophic support (Kinrade *et al.*, 2001). In the mature cord, we found that both LG and longitudinal axons were medially misplaced to the CNS midline in *jing* hemizygotes and after glial knockdown of *jing* and *DATR-X* (Figure 7, H–J, M, N). Despite the maintenance of glial–axonal contact, the numbers of total glia steadily decreased during embryogenesis in *jing* and *DATR-X* glial mutants (Figure 7O). However, glial numbers were unaffected after neuronal-specific

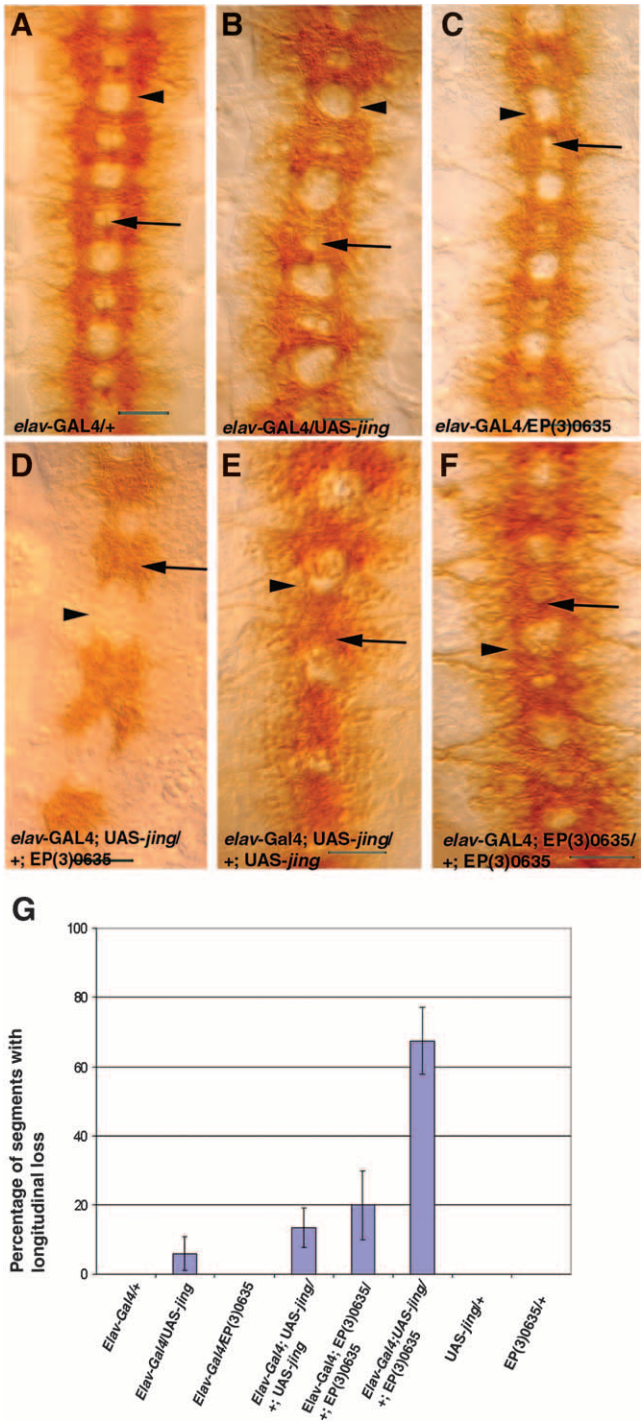

Figure 5.—Pan-neural expression of *DATR-X* and *jing* in embryonic CNS neurons synergistically affects axon patterning. Ventral views of the ventral nerve cord (VNC) of stage 15 embryos stained with BP102 (A–F) and shown with anterior up. (A) Control embryo heterozygous for *elav*-Gal4 and w^{1118}. Thick longitudinal connectives connect each hemisegment (arrowhead). The arrow denotes the space between the anterior and posterior commissural axons. (B and C) After overexpression of *jing* (B) or *DATR-X* (C) in postmitotic CNS neurons, longitudinal axons (arrowheads) are very thin and the space between commissural axons is smaller (arrows). (D) Coexpression of one copy of EP(3)0635 and UAS-*jingE* in postmitotic neurons has synergistic effects. Note the absence of longitudinal connectives (arrowhead). (E and F) Additive effects of overexpressing two copies of *UAS-jingE* (E) or EP(3)0635 (F) Note that commissural axons are often not separated (arrows) and longitudinal connectives are very thin (arrowheads). (G) Quantitative analysis of longitudinal connective formation. Bars, 50 μm.

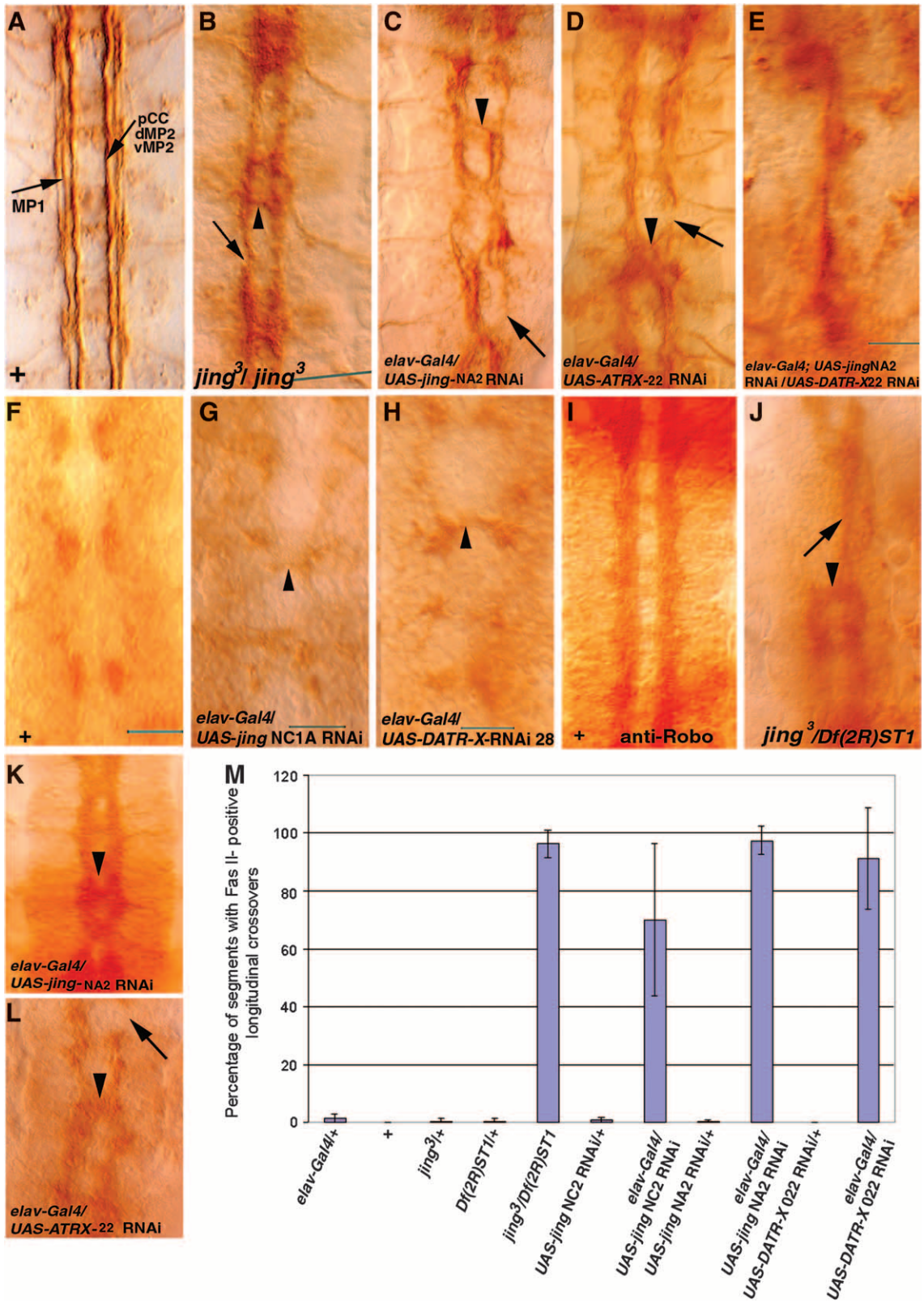

FIGURE 6.—*DATR-X* and *jing* functions are required specifically in CNS neurons for longitudinal connective formation. *DATR-X* and *jing* RNAi transgene expression was driven in neurons by *ELAV-Gal4*. (A–E and F–L) Shown are close-up views of the VNC of whole-mount stage16 embryos stained with anti-Fasciclin II monoclonal antibody (1D4) (A–E) and anti-Robo (F–L). Stage 12 embryos stained with anti-Robo (F–H). (A) In wild-type embryos, three longitudinal fascicles are clearly delineated. (B–D) In *jing* (B and C) and *DATR-X* (D) mutants, longitudinal fascicles misroute across the midline (arrowheads) and are broken (arrows). (E) After coexpression of *jing* and *DATR-X* RNAi transgenes in neurons, longitudinal fascicles fuse into one tract at the midline.

(*continued*)

jing and *DATR-X* knockdown despite a medial misplacement and mispositioning of LG (Figure 7, K, L, O). Therefore, *jing* and *DATR-X* glial-specific mutations perturb an autonomous survival function that cannot be compensated for by axon contact.

DISCUSSION

A conserved role for ATR-X in the embryonic CNS? Of the candidates from the screen, we chose to further study *DATR-X* due to a possible involvement in Jing CNS function and disease relevance. Mutations in the human *ATR-X* gene are associated with several X-linked MR phenotypes that lead to cognitive delay, facial dysmorphism, microcephaly, skeletal and genital abnormalities, and neonatal hypotonia (Gibbons *et al.* 1995a,b; Villard *et al.* 1996a,b; Gibbons and Higgs 2000). A total of 87% of MR genes have a fruit fly homolog and 76% have a candidate functional ortholog revealing a remarkable conservation between humans and *D. melanogaster* (Inlow and Restifo 2004). Some orthologs of human MR genes have cellular phenotypes involving neurons, glia, and neural precursor cells and arise from defects in proliferation, migration, and process extension or arborization (Inlow and Restifo 2004). For example, targeted mutation of ATR-X to the early forebrain in mice leads to cortical progenitor cell death and reduced forebrain size (Bérubé *et al.* 2005). In addition, mutations in genes controlling the identity of forebrain neuronal precursors can result in holoprosencephaly in which the brain hemispheres do not separate (Wallis and Muenke 2000). An increased understanding of the molecular and cellular bases for hereditary MR is critical for the generation of drug treatments.

ATR-X belongs to the SWI/SNF group of chromatin remodeling proteins, which use the energy provided by ATP hydrolysis to disrupt histone–DNA associations and move nucleosomes to different positions (Kingston and Narlikar 1999; Whitehouse *et al.* 1999). This chromatin modulation allows for the access of activators or repressors to their DNA binding sites in their target genes. The helicase C and SNF2N domains of ATR-X have been shown to have DNA translocase and nucleosome-remodeling activities (Xue *et al.* 2003; Tang *et al.* 2004). Accordingly, mutations in ATR-X have been mapped to the helicase C and SNF2N domains, which show ~60% homology with those in *DATR-X* and have been conserved from *C. elegans* to humans. This conservation supports a conserved role for Drosophila ATR-X in chromatin remodeling (Tang *et al.* 2004; this work).

Vertebrate ATR-X has a C_2C_2 zinc-finger motif in the amino terminus that is similar to a plant homeodomain finger previously identified in proteins involved in chromatin-mediated transcriptional regulation (Aasland *et al.* 1995; Gibbons *et al.* 1997). Interestingly, *D. melanogaster* and *C. elegans* ATR-X proteins do not contain the zinc-finger domain, suggesting that these structures may have been acquired through evolution due to a necessity in vertebrate chromatin remodeling mechanisms. Patients have been identified with mutations in the ATPase and zinc-finger domains of ATR-X, confirming that these are essential functional regions of the protein (Villard *et al.* 1996b,c; Gibbons and Higgs 2000).

Given the absence of the zinc-finger domains in *DATR-X*, we postulate that invertebrate *DATR-X* proteins may be complexed with proteins containing a nuclear targeting and DNA-binding motif to regulate gene expression at the proper regulatory sites. This may be one role of Jing since it has an embryonic expression pattern as well as mutant and overexpression phenotypes very similar to those of *DATR-X*. Therefore, it seems that the ATPase domain of *DATR-X* has been conserved through evolution and that the other regions of the protein may have evolved to suit the specific needs of the cell. In summary, different mechanisms of ATR-X function and different binding partners across species may account for the divergence of sequence with respect to the amino terminal and Q-rich repeats while the main chromatin remodeling aspects of ATR-X remain similar.

Jing encodes a nuclear protein with putative DNA-binding and transcriptional regulatory domains (Liu and Montell 2001; Sedaghat *et al.* 2002). The C_2H_2 zinc fingers of Jing are most similar (50% identical) to those of the mouse adipocyte enhancer binding protein 2 (AEBP2) and also show 25% homology to those of the Krüppel family of transcription factors, including those encoding *gli* and *ZIC2* (Liu and Montell 2001). AEBP2 function is implicated in chromatin remodeling events (Cardoso *et al.* 1998; Cao and Zhang 2004) and has strong expression in the brain (He *et al.* 1999).

Genetic screening identifies a related group of *jing*-interacting genes: We have utilized a background sensitive to *jing* function to conduct a genetic screen in the eye. For the GOF screen, we hypothesized that misexpression of *jing* in the eye in combination with other genes involved in *jing* transcriptional regulation would lead to alterations in gene expression and consequently disrupt ommatidial formation. The genetic relationship between *DATR-X* and *jing* in embryonic neurons and glia shows that the screen was

(F) Wild-type Robo-positive glia are present on each side of the midline. (G and H) Medial misplacement of Robo-positive glia (arrowheads) occurs after neuronal-specific knockdown of *jing* and *DATR-X*. (I) Lateral positioning of Robo-positive axons in wild-type embryos. (J–L) Robo-positive axons cross the midline (arrowheads) after neuronal-specific knockdown of *DATR-X* and *jing*. Axonal breaks are evident (arrow in L). Arrow in J denotes remaining connective. (M) Graph displaying the average number of longitudinal axons that cross over the CNS midline per embryo.

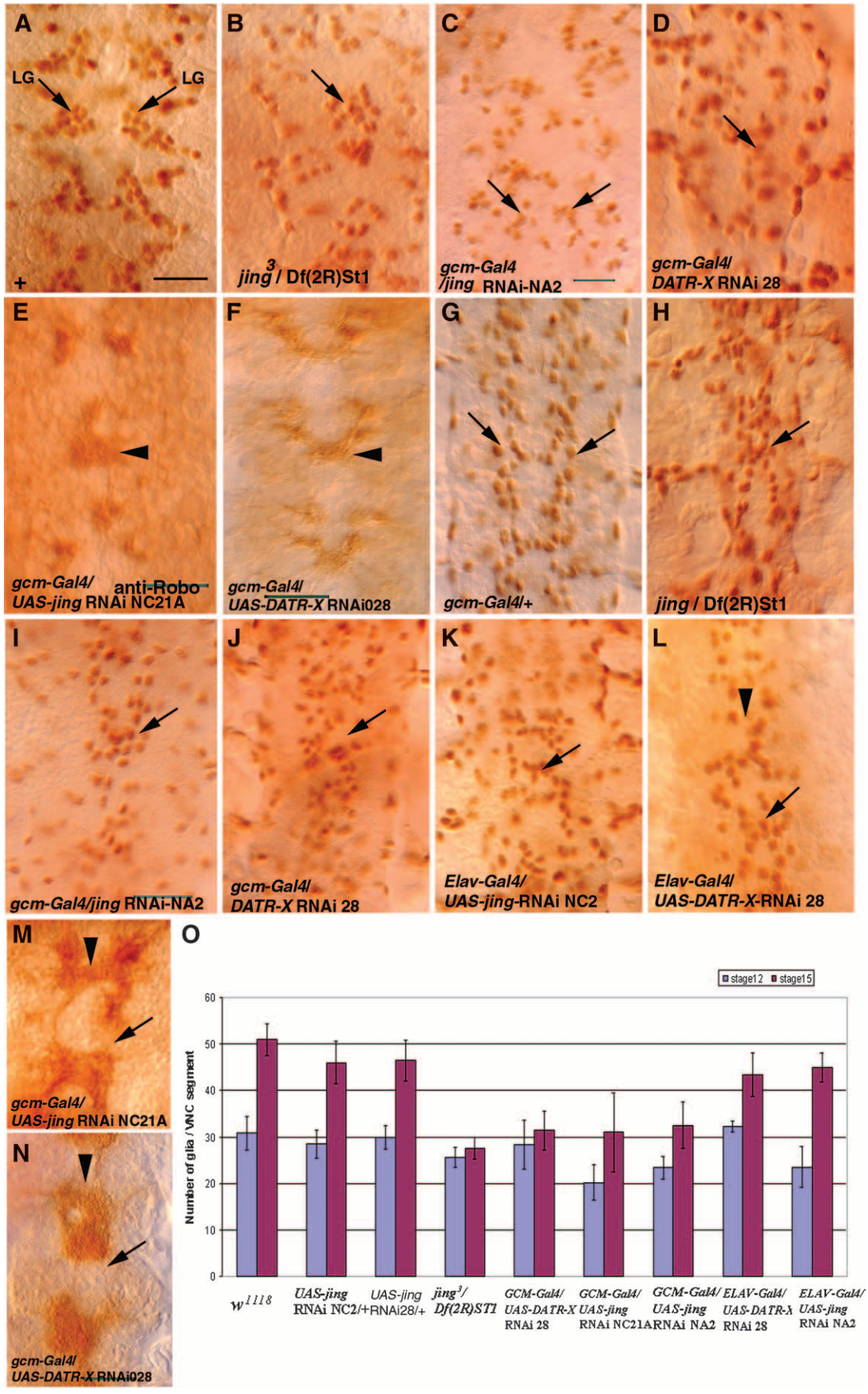

FIGURE 7.—*DATR-X* and *jing* are required for glial patterning and survival. (A–D and G–L) CNS glia were identified in

(*continued*)

successful in identifying genes whose function in adult neuronal cells is relevant to *jing* function in the embryonic CNS. This is consistent with previous findings that the fly eye is a valid system for targeting genes that function in other tissues (Raymond *et al.* 2004).

EP(3)3084 contains a transposon in proximity to a novel gene known by its FlyBase transcript identifier as CG15507. Despite strong effects of EP(3)3084 expression in the eye these were specifically strongly enhanced after coexpression with *jing*, *DAtx2*, and *JIGR1*. Furthermore, each gene specifically interacted with each other but not with randomly chosen EP lines, suggesting a functional relationship between the four genes. The EP elements in these lines are located in the 5′ untranslated region of the downstream genes, suggesting they may result in overexpression (BDGP). Given the regulatory role of MADF domains, it is possible that JIGR1 regulates gene expression with Jing and *DATR-X* (England *et al.* 1992; Bhaskar and Courey 2002). Alternatively, JIGR1 may regulate the expression of a Jing/DATR-X target gene. Likewise, DAtx2 may be involved in regulating the translation of a protein that is an essential component of a Jing/DATR-X/JIGR1 complex or a downstream target of these genes (Satterfield *et al.* 2002; Ciosk *et al.* 2004). A role for the orthologs of translational regulators in MR has been shown for the Drosophila ortholog of fragile-X MR 1 (*Dfmr1*). *Dfmr1* regulates the MAP1B homolog of Futsch to control synaptic structure and function in the embryonic Drosophila CNS (Zhang *et al.* 2001). Therefore, genetic screening and phenotypic analysis in Drosophila have the power to decipher pathways and the cellular bases of MR genes.

Neuronal and glial functions of *jing* and *DATR-X* dictate axon tract formation: In wild-type Drosophila embryos, LG assume characteristic positions and do not cross the midline or into adjacent VNC segments (Ito *et al.* 1995). This is due to multiple mechanisms at different stages of development, including response to repulsive and attractive molecules, cell–cell contact, trophic support, and axon contact (Kinrade *et al.*, 2001). A disruption in any of these processes will perturb formation of the glial and axonal scaffolds. The expression of *jing* and *DATR-X* reporter genes in LG correlates with the LG phenotypes associated with mutations in these genes.

During stage 12, Robo present on the LG responds to repulsive midline Slit molecules to maintain lateral positioning (Kinrade *et al.* 2001). The medial misplacement of Robo- and Repo-positive LG during stage 12 after *jing* and *DATR-X* glial-specific knockdown suggests that there may have been a breakdown in Robo-dependent repulsive mechanisms. However, the fact that Robo protein was present after *jing* and *DATR-X* glial and neuronal knockdown suggests that *robo* expression may not be regulated by Jing and *DATR-X*. Alternatively, Jing and *DATR-X* may regulate the expression of a factor that controls how Robo reads the Slit signal. In support, misrouting of axons across the midline in the presence of Robo occurs in *calmodulin* and *Son of sevenless* mutants where these proteins are required to process the Sli signal (Fritz and VanBerkum 2000). It is also possible that *jing* and *DATR-X* regulate the expression of factors controlling glial and neuronal positioning in a Robo-independent fashion (Kinrade *et al.* 2001).

jing and *DATR-X* mutations clearly affect more than Robo-mediated LG positioning. First, glial survival is not affected in *robo* mutant embryos, whereas glia die despite continuous axonal contact in *jing* and *DATR-X* glial-specific mutants. Therefore, the loss of CNS glia may reflect a breakdown in an intrinsic survival pathway mediated by *jing* and *DATR-X*. The expression of *jing* and *DATR-X* reporter genes in glia is consistent with such a role. Furthermore, both *jing* and *DATR-X/ATR-X* have been implicated in cell survival processes in the CNS midline and tracheal cells and in cortical progenitors, respectively (Sedaghat *et al.* 2002; Sonnenfeld *et al.* 2004; Bérubé *et al.* 2005).

Second, in *robo* mutants only the central pCC/MP2 fascicle, but not the outer two longitudinal fascicles, is affected. However, in *jing* and *DATR-X* glial and neuronal mutants the outer fascicles are fused, often broken, and can be seen crossing the midline. These defects are similar to those after ablation of neurons or glia and after genetic loss of glia as in *gcm* mutants (Hosoya *et al.* 1995; Jones *et al.* 1995; Vincent *et al.* 1996; Hidalgo and Brand 1997). These observations suggest that multiple biological processes require the proper function of these genes and are consistent with an important upstream role for *jing* and *DATR-X* in glial and neuronal differentiation.

whole-mount embryos stained with anti-Repo. (E, F, M, and N) Embryos stained with anti-Robo. Shown are close-up ventral views of the nerve cord of stage 12/3 (A–F) and stage 15 (G–N) embryos. (A) In wild-type stage 12/3 embryos, longitudinal glia (LG) have already migrated medially to their positions to guide pioneer longitudinal axons. (B–D) In contrast, LG inappropriately occupy positions at the CNS midline in hemizygous *jing* embryos (B) and in those with glial-specific knockdown of *jing* (C) and *DATR-X* (D) as driven by *gcm-Gal4*. (E and F) Robo-positive glia are misplaced medially after expression of *jing* (E) and *DATR-X* (F) RNAi transgenes in CNS glia. (G) In wild-type embryos, the LG occupy a two-cell wide row lining the longitudinal connectives (arrows). The LG are observed only in the dorsal plane of view. (H–J) In *jing* hemizygotes (H) and in *jing* (I) and *DATR-X* (J), glial mutants glia are misplaced across the midline (arrows). (K and L) In *jing* (K) and *DATR-X* (L) neuronal mutants, glia cross the midline but are also scattered in the nerve cord. (M and N) Glial knockdown of *jing* (M) and *DATR-X* (N) results in breaks in Robo-positive longitudinal axons (arrows) and inappropriate midline crossings (arrowheads). (N) Quantitative analysis of glia during stages 12 and 15 after expressing *jing* and *DATR-X* RNAi transgenes in glia or neurons. Bars, 50 μm.

Evidence is accumulating that chromatin accessibility plays a key role in the transcriptional regulation of cell-type-specific gene expression in the CNS (Hsieh *et al.* 2004). The conservation in ATPase domains along with the similar phenotype of *DATR-X* and *jing* mutations and in their expression patterns raises the possibility that Jing is involved in the targeting of a chromatin remodeling complex containing *DATR-X* to transcriptional target genes whose products are required for the response of longitudinal growth cones and glia to guidance cues.

In summary, we have identified a group of genes that pertain to *jing* function and specifically genetically interact in adult neuronal cells. Our results show that specific neural and glial developmental defects underlie the problems in axon guidance associated with mutations in *DATR-X* and *jing*. More studies using targeted mutations of MR genes will alleviate the view that brain phenotypes result from generic effects due to a heightened sensitivity of the brain.

We thank Marc Freeman for *gcm*-gal4 and S. Hayashi for *btl*-gal4. We thank Doug Holmyard at the Bioimaging Centre at Mount Sinai Hospital for performing SEM. We thank Helga Agah for help with immunohistochemistry. We thank Andrew Ridsdale and the OGHRI for use of the confocal microscope and training. This work was supported by a grant from the Canadian Institutes of Health Research to M.S.

LITERATURE CITED

Aasland, R., T. J. Gibson and A. F. Stewart, 1995 The PHD finger: implications for chromatin-mediated transcriptional regulation. TIBS **20:** 56–59.

Abidi, F., N. J. Carpenter, L. Villard, M. Curtis, M. Fontes *et al.*, 1999 The Carpenter-Waziri syndrome results from a mutation in *D*ATR-X. Am. J. Med. Genet. **85:** 249–251.

Adams, M. D., S. E. Celniker, R. A. Holt, C. A. Evans, J. D. Gocayne *et al.*, 2000 The genome sequence of *Drosophila melanogaster*. Science **5461:** 2185–2195.

Ahmad, K., and S. Henikoff, 2001 Modulation of a transcription factor counteracts heterochromatic gene silencing in *Drosophila*. Cell **104:** 839–847.

Aravind, L., 2000 The BED finger, a novel DNA-binding domain in chromatin- boundary-element-binding proteins and transposases. Trends Biochem. Sci. **25:** 421–423.

Ashburner, M., 1989 *Drosophila*: *A Laboratory Manual*. Cold Spring Harbor Laboratory Press, Cold Spring Harbor, NY.

Ashley, C. T., C. G. Pendleton, W. W. Jennings, A. Saxena and C. V. Glover, 1989 Isolation and sequencing of cDNA clones encoding *Drosophila* chromosomal protein D1. A repeating motif in proteins which recognize at DNA. J. Biol. Chem. **264:** 8394–8401.

Bate, C. M., and E. B. Grunewald, 1981 Embryogenesis of an insect nervous system II: a second class of neuron precursor cells and the origin of the intersegmental connectives. J. Embryol. Exp. Morphol. **61:** 317–330.

Barresi, M. J. F., L. D. Hutson, C-B. Chien and R. O. Karlstrom, 2005 Hedgehog regulated Slit expression determines commissure and glial cell position in the zebrafish forebrain. Development **132:** 3643–3656.

Battye, R., A. Stevens and J. R. Jacobs, 1999 Axon repulsion from the midline of the *Drosophila* CNS requires slit function. Development **126:** 2475–2481.

Bérubé, N. G., M. Mangelsdorf, M. Jagla, J. Vanderluit, D. Garrick *et al.*, 2005 The chromatin-remodeling protein ATRX is critical for neuronal survival during corticogenesis. J. Clin. Invest. **115:** 258–267.

Bhaskar, V., and A. J. Courey, 2002 The MADF-BESS domain factor Dip3 potentiates synergistic activation by Dorsal and Twist. Gene **299:** 173–184.

Bhat, K. M., 2005 Slit-Roundabout signaling neutralizes netrin–frazzled-mediated attractant cue to specify the lateral positioning of longitudinal axon pathways. Genetics **170:** 149–159.

Booth, G. E., E. F. Kinrade and A. Hidalgo, 2000 Glia maintain follower neuron survival during *Drosophila* CNS development. Development **127:** 237–244.

Brand, A. H., and N. Perrimon, 1993 Targeted gene expression as a means of altering cell fates and generating dominant phenotypes. Development **118:** 401–415.

Brody, T., C. Stivers, J. Nagle and W. F. Odenwald, 2002 Iden tification of novel *Drosophila* neural precursor genes using a differential embryonic head cDNA screen. Mech. Dev. **113:** 41–59.

Campbell, G., H. Goring, T. Lin, E. Spana, S. Anderson *et al.*, 1994 RK2, a glila-specific homeodomain protein required for embryonic nerve cord condensation and viability in *Drosophila*. Development **120:** 2957–2966.

Cao, R., and Y. Zhang, 2004 SUZ12 is required for both the histone methyltransferase activity and the silencing function of the EED-EZH2 complex. Mol. Cell **15**(1): 57–67.

Cardoso, C., S. Timsit, L. Villard, M. Khrestchatisky, M. Fontes *et al.*, 1998 Specific interaction between the ATR-X gene product and the SET domain of the human EZH2 protein. Hum. Mol. Genet. **7:** 679–684.

Cardoso, C., Y. Lutz, C. Mignon, E. Compe, D. Depetris *et al.*, 2000 ATR-X mutations cause impaired nuclear location and altered DNA binding properties of the ATR-X protein. J. Med. Genet. **37:** 746–751.

Ciosk, R., M. DePalma and J. R. Priess, 2004 ATX-2, the *C. elegans* ortholog of ataxin 2, functions in translational regulation in the germline. Development **131:** 4831–4841.

Cutler, G., K. M. Perry and R. Tjian, 1998 Adf-1 is a nonmodular transcription factor that contains a TAF-binding Myb-like motif. Mol. Cell Biol. **18:** 2252–2261.

Dearborn, R., Jr., and S. Kunes, 2004 An axon scaffold induced by retinal axons directs glia to destinations in the *Drosophila* optic lobe. Development **131:** 2291–2303.

England, B. P., A. Admon and R. Tjian, 1992 Cloning of the *Drosophila* transcription factor Adf-1 reveals homology to Myb oncoproteins. Proc. Natl. Acad. Sci. USA **89:** 683–687.

Ewel, A., J. R. Jackson and C. Benyajati, 1990 Alternative DNA-protein interactions in variable-length internucleosomal regions associated with *Drosophila Adh* distal promoter expression. Nucleic Acids Res. **18:** 1771–1781.

Freeman, M. R., J. Delrow, J. Kim, E. Johnson and C. Q. Doe, 2003 Unwrapping glial biology: Gcm target genes regulating glial development, diversification and function. Neuron **38:** 567–580.

Fritz, J. L., and M. F. VanBerkum, 2000 Calmodulin and son of sevenless dependent signaling pathways regulate midline crossing of axons in the Drosophila CNS. Development **27**(9): 1991–2000.

Gibbons, R. J., and D. R. Higgs, 2000 Molecular-clinical spectrum of the ATR-X syndrome. Am. J. Med. Genet. **97:** 204–212.

Gibbons, R. J., L. Brueton, V. J. J. Buckle Burn, J. Clayton-Smith, B. C. C. Davison *et al.*, 1995a The clinical and hematological features of the X-linked α-thalassemia/mental retardation syndrome (ATR-X). Am. J. Med. Genet. **55:** 288–299.

Gibbons, R. J., D. J. Picketts, L. Villard and D. R. Higgs, 1995b Mutations in a putative global transcriptional regulator cause X-linked mental retardation with α-thalassemia (ATR-X syndrome). Cell **80:** 837–845.

Gibbons, R. J., S. Bachoo, D. J. Picketts, S. Aftimos, B. Asenbauer *et al.*, 1997 Mutations in transcriptional regulator ATRX establish the functional significance of a PHD-like domain. Nat. Genet. **17:** 146–148.

Halter, D. A., J. Urban, C. Rickert, S. S. Ner, K. Ito *et al.*, 1995 The homeobox gene *repo* is required for the differentiation and maintenance of glia function in the embryonic nervous system of *Drosophila*. Development **121:** 317–332.

Hammond, S. M., A. A. Caudy and G. J. Hannon, 2001 Post-transcriptional gene silencing by double-stranded RNA. Nat. Rev. Genet. **2**(2): 110–119.

Hay, B. A., T. Wolff and G.M. Rubin, 1994 Expression of baculovirus P35 prevents cell death in *Drosophila*. Development **120:** 2121–2129.

He, G.-P., S. Kim and H.-S. Ro, 1999 Cloning and characterization of a novel zinc finger transcriptional repressor. J. Biol. Chem. **274:** 14678–14684.

Hidalgo, A., and A. H. Brand, 1997 Targeted neuronal ablation: the role of pioneer neurons in guidance and fasciculation in the CNS of *Drosophila*. Development **124:** 3253–3262.

Hidalgo, A., and G. Booth, 2000 Glia dictate trajectories of pioneer neurons in the *Drosophila* embryonic CNS. Development **127:** 393–402.

Hidalgo, A., E. F Kinrade and M. Georgiou, 2001 The *Drosophila* neuregulin vein maintains glial survival during axon guidance in the CNS. Dev. Cell **1:** 679–690.

Hosoya, T., K. Takizawa, K. Nitta and Y. Hotta, 1995 Glial cells missing: a binary switch between neuronal and glial determination in *Drosophila*. Cell **82:** 1025–1036.

Hsieh, J., K. Nakashima, T. Kuwabara, E. Mejia and F. H. Gage, 2004 Histone deacetylase inhibition-mediated neuronal differentiation of multipotent adult neural progenitor cells. Proc. Natl. Acad. Sci. USA **101:** 16659–16664.

Huang, Y., S. J. Myers and R. Dingledine, 1999 Transcriptional repression by REST: recruitment of Sin3A and histone deacetylase to neuronal genes. Nat. Neurosci. **2**(10): 867–872.

Hulo, N., C. J. A. Sigrist, V. Le Saux, P. S. Langendijk-Genevaux, L. Bordoli *et al.*, 2004 Recent improvements to the PROSITE database. Nucleic Acids Res. **32:** D134–D137.

Inlow, J. K., and L. L. Restifo, 2004 Molecular and comparative genetics of mental retardation. Genetics **166:** 835–881.

Ito, K., J. Urban and G. M. Technau, 1995 Distribution, classification and development of *Drosophila* glial cells in the late embryonic and early larval ventral nerve cord. Roux's Arch. Dev. Biol. **204:** 284–307.

Jacobs, J. R., and C. S. Goodman, 1989 Embryonic development of axon pathways in the *Drosophila* CNS. II. Behavior of pioneer growth cones. J. Neurosci. **9:** 2402–2411.

Janody, F., J. Reischl and N. Dostatni, 2000 Persistence of Hunchback in the terminal region of the *Drosophila* blastoderm embryo impairs anterior development. Dev. **127:** 1573–1582.

Jones, B. W., R. D. Fetter, G. Tear and C. S. Goodman, 1995 Glial cells missing: a genetic switch that controls glial versus neuronal fate. Cell **82:** 1013–1023.

Keleman, K., S. Rajagopalan, D. Cleppien, D. Teis, K. Palha *et al.*, 2002 Comm sorts Robo to control axon guidance at the *Drosophila* midline. Cell **110:** 415–427.

Keleman, K., C. Ribeiro and B. J. Dickson, 2005 Comm function in commissural axon guidance: cell-autonomous sorting of Robo in vivo. Nat. Neurosci. **8:** 156–163.

Kidd, T., K. Brose, K. J. Mitchell, R. D. Fetter, M. Tessier-Lavigne *et al.*, 1998a Roundabout controls axon crossing of the CNS midline and defines a novel subfamily of evolutionary conserved guidance receptors. Cell **92:** 205–215.

Kidd, T., C. Russell, C. S. Goodman and G. Tear, 1998b Dosage-sensitive and complementary functions of roundabout and commissureless control axon crossing of the CNS midline. Neuron **20:** 25–33.

Kidd, T., K. S. Bland and C. S. Goodman, 1999 Slit is the midline repellent for the Robo receptor in *Drosophila*. Cell **96:** 785–794.

Kingston, R. E., and G. J. Narlikar, 1999 ATP-dependent remodeling and acetylation as regulators of chromatin fluidity. Genes Dev. **13:** 2339–2352.

Kinrade, E. F. V., T. Brates, G. Tear, and A. Hidalgo, 2001 Round about signaling, cell contact and trophic support confine longitudinal glia and axons in the *Drosophila* CNS. Development **128:** 207–216.

Lasko, P., 2000 The *Drosophila* melanogaster genome: translation factors and RNA binding proteins. J. Cell Biol. **150:** F51–F56.

Lee, Y. S., and R. W. Carthew, 2003 Making a better RNAi vector for *Drosophila*: use of intron spacers. Methods **30:** 322–329.

Letunic, I., R. R. Copley, S. Schmidt, F. D. Ciccarelli, T. Doerks *et al.*, 2004 SMART 4.0: towards genomic data integration. Nucleic Acids Res. **32:** D142–D144.

Liu, Y., and D. J. Montell, 2001 *jing*: a downstream target of *slbo* required for developmental control of border cell migration. Development **128:** 321–330.

Long, H., C. Sabatier, L. Ma, A. Plump, W. Yuan *et al.*, 2004 Conserved roles for Slit and Robo proteins in midline commissural axon guidance. Neuron **42:** 213–223.

Oland, L. A., and L. P. Tolbert, 2002 Key interactions between neurons and glial cells during neural development in insects. Annu. Rev. Entomol. **48:** 89–110.

Page-McCaw, P. S., K. Amonlirdviman and P. A. Sharp, 1999 PUF60: a novel U2AF65-related splicing activity. RNA **5:** 1548–1560.

Pena-Rangel, M. T., I. Rodriguez and J. R. Riesgo-Escovar, 2002 A misexpression study examining dorsal thorax formation in *Drosophila melanogaster*. Genetics **160:** 1035–1050.

Picketts, D. J., D. R. Higgs, S. Bachoo, D. J. Blake, O. W. J. Quarrell *et al.*, 1996 *ATRX* encodes a novel member of the SNF2 family of proteins: mutations point to a common mechanism underlying the ATR-X syndrome. Hum. Mol. Genet. **5:** 1899–1907.

Rajagopalan, S., E. Nicolas, V. Vivancos, J. Berger and B. J. Dickson, 2000a Crossing the midline. Roles and regulation of Robo receptors. Neuron **28:** 767–777.

Rajagopalan, S., V. Vivancos, E. Nicolas and B. J. Dickson, 2000b Selecting a longitudinal pathway. Robo receptors specify the lateral position of axons in the *Drosophila* CNS. Cell **103:** 1033–1045.

Rasband, K., M. Hardy and C. B. Chien, 2003 Generating X: formation of the optic chiasm. Neuron **39:** 885–888.

Raymond, K., E. Bergeret, A. Avet-Rochex, R. Griffin-Shea and M.-O. Fauvarque, 2004 A screen for modifiers of RacGAP(84C) gain-of-function in the *Drosophila* eye revealed the LIM kinase Cdi/TESK1 as a downstream effector of Rac1 during spermatogenesis. J. Cell Sci. **117:** 2777–2789.

Robinow, S., and K. White, 1988 The locus *ELAV* of *Drosophila melanogaster* is expressed in neurons at all developmental stages. Dev. Biol. **126:** 294–303.

Rodriguez-Alfageme, G. T., G. T. Rudkin and L. Cohen, 1980 Isolation, properties and cellular distribution of D1, a chromosomal protein of *Drosophila*. Chromosoma **78:** 1–31.

Rørth, P., 1996 A modular misexpression screen in *Drosophila* detecting tissue- specific phenotypes. Proc. Natl. Acad. Sci. USA **93:** 12418–12422.

Rubin, G. M., 1988 *Drosophila melanogaster* as an experimental organism. Science **240:** 1453–1459.

Rubin, G. M., and A. C. Spradling, 1983 Vectors for P element-mediated gene transfer in *Drosophila*. Nucleic Acids Res. **11:** 6341–6351.

Rubin, G. M., L. Hong, P. Brokstein, M. Evans-Holm, E. Frise *et al.*, 2000 A *Drosophila* complementary DNA resource. Science **5461:** 2222–2224.

Satterfield, T. F., S. M. Jackson and L. J. Pallanck, 2002 A *Drosophila* homolog of the polyglutamine disease gene *SCA2* is a dosage-sensitive regulator of actin filament formation. Genetics **162:** 1687–1702.

Sedaghat, Y., W. Miranda and M. Sonnenfeld, 2002 The jing Zn finger transcription factor is a mediator of cellular differentiation in the *Drosophila* CNS midline and trachea. Development **129:** 2591–2606.

Seeger, M., G. Tear, D. Ferres-Marco and C. S. Goodman, 1993 Mutations affecting growth cone guidance in *Drosophila*: genes necessary for guidance toward or away from the midline. Neuron **10:** 409–426.

Shiga, Y., M. Tanada-Matakatsu and S. A. Hayashi, 1996 Nuclear β-galactosidase fusion protein as a marker of morphogenesis in living *Drosophila*. Dev. Growth Differ. **38:** 99–106.

Simpson, J. H., K. S. Bland, R. D. Fetter and C. S. Goodman, 2000a Short-range and long-range guidance by Slit and its Robo receptors: a combinatorial code of Robo receptors controls lateral position. Cell **103**(7): 1019–1032.

Simpson, J. H., T. Kidd, K. S. Bland and C. S. Goodman, 2000b Short-range and long-range guidance by Slit and its Robo receptors: Robo and Robo2 play distinct roles in midline guidance. Neuron **28:** 753–766.

Sonnenfeld, M. J., N. Barazesh, Y. Sedaghat and C. Fan, 2004 The *jing* and *ras1* pathways are functionally related during CNS midline and tracheal development. Mech. Dev. **121:** 1531–1547.

Tang, J., S. Wu, H. Liu, R. Stratt, O. G. Barak *et al.*, 2004 A novel transcription regulatory complex containing death domain-associated protein and the ATR-X syndrome protein. J. Biol. Chem. **279:** 20369–20377.

Tatusova, T. A., and T. L. Madden, 1999 Blast 2 sequences-a new tool for comparing protein and nucleotide sequences. FEMS Microbiol. Lett. **174:** 247–250.

Tear, G., R. Harris, S. Sutaria, K. Kilomanski, C. S. Goodman *et al.*, 1996 Commissureless controls growth cone guidance across the

CNS midline in Drosophila and encodes a novel membrane protein. Neuron **16:** 501–514.

Tessier-Lavigne, M., 1994 Axon guidance by diffusible repellants and attractants. Curr. Opin. Genet. Dev. **4:** 596–601.

Tessier-Lavigne, M., and C. S. Goodman, 1996 The molecular biology of axon guidance. Science **274:** 1123–1133.

Tseng, A. S., and I. K. Hariharan, 2002 An overexpression screen in Drosophila for genes that restrict growth or cell-cycle progression in the developing eye. Genetics **162:** 229–243.

VanVactor, D., H. Sink, D. Fambrough, R. Tsoo and C. S. Goodman, 1993 Genes that control neuromuscular specificity in *Drosophila*. Cell **73:** 1137–1153.

Villard, L., A. Toutain, A. M. Lossi, J. Gecz, C. Houdayer *et al.*, 1996a Splicing mutation in the *ATR-X* gene can lead to a dysmorphic mental retardation phenotype without α-thalassemia. Am. J. Hum. Genet. **58:** 499–505.

Villard, L., P. Saugier-Veber, J. Gecz, J. F. Mattei, A. Munnich *et al.*, 1996b *ATR-X* mutation in a large family with Juberg-Marsidi syndrome. Nat. Genet. **12:** 359–360.

Villard, L., J. Gecz, J. F. Mattei, M. Fontes, P. Saugler-Veber *et al.*, 1996c *ATR-X* mutation in a large family with Juberg-Marsidi syndrome. Nat. Genet. **4:** 316–320.

Villard, L., M. Fontès and J. J. Ewbank, 1999 Characteriztion of *ATR-X-1*, a *Caenorhabditis elegans* gene similar to the human ATR-X gene. Gene **236:** 13–19.

Vincent, S., J. L. Vonesch and A. Giangrande, 1996 Glide directs glial fate commitment and cell fate switch between neurons and glia. Development **122:** 131–139.

Wallis, D., and M. Muenke, 2000 Mutations in holoprosencephaly. Hum. Mutat. **16**(2): 99–108.

Whitehouse, I., A. Flaus, B. R. Cairns, M. F. White, J. L. Workman *et al.*, 1999 Nucleosome mobilization catalysed by the yeast SWI/SNF complex. Nature **400:** 784–787.

Whitington, P. M., C. Quilkey and H. Sink, 2004 Necessity and redundancy of guidepost cells in the embryonic *Drosophila* CNS. Int. J. Dev. Neurosci. **22:** 157–163.

Wing, J. P., B. A. Schreader, T. Yokokura, Y. Wang, P. S. Andrews *et al.*, 2002 *Drosophila* Morgue is an F box/ubiquitin conjugase domain protein important for grim-reaper mediated apoptosis. Nat. Cell Biol. **6:** 451–456.

Xiong, W. C., H. Okano, N. H. Patel, J. A. Blendy and C. Montell, 1994 Repo encodes a glial-specific homeo domain protein required in the *Drosophila* nervous system. Genes Dev. **8:** 981–994.

Xue, Y., R. Gibbons, Z. Yan, D. Yang, T. L. McDowell *et al.*, 2003 The ATRX syndrome protein forms a chromatin-remodeling complex with Daxx and localizes in promyelocytic leukemia nuclear bodies. Proc. Natl. Acad. Sci. USA **100:** 10635–10640.

Yao, K.-M., and K. White, 1994 Neural specificity of *ELAV* expression: defining a *Drosophila* promoter for directing expression to the nervous system. J. Neurochem. **63:** 41–51.

Zhang, Y. Q., A. M. Bailey, H. J. Matthies, R. B. Renden, M. A. Smith *et al.*, 2001 *Drosophila* fragile X-related gene relates the MAP1B homolog Futsch to control synaptic structure and function. Cell **107:** 591–603.

Zipursky, S. L., and G. M. Rubin, 1994 Determination of neuronal cell fate: lessons from the R7 neuron of *Drosophila*. Annu. Rev. Neurosci. **17:** 373–397.

Communicating editor: K. V. Anderson